2013

DEPARTAMENTO DE CIÊNCIAS DA VIDA

FACULDADE DE CIÊNCIAS E TECNOLOGIA
UNIVERSIDADE DE COIMBRA

Effect of methamphetamine on microglial and endothelial cells: nitrosative and oxidative stress responses.

Cláudia Sofia Aguiar Amaral

2013

Effect of methamphetamine on mecroglial and endotelial cells: nitrosative and oxidative stress

Cláudia Amaral

DEPARTAMENTO DE CIÊNCIAS DA VIDA

FACULDADE DE CIÊNCIAS E TECNOLOGIA
UNIVERSIDADE DE COIMBRA

Effect of methamphetamine on microglial and endotelial cells: nitrosative and oxidative stress

Dissertação apresentada à Universidade de Coimbra para cumprimento dos requisitos necessários à obtenção do grau de Mestre em Bioquímica, realizada sob a orientação científica da Professora Doutora Ana Paula Silva (Universidade de Coimbra) e supervisão da FCTUC pelo Professor Doutor Armando Cristovão (Universidade de Coimbra).

Cláudia Sofia Aguiar Amaral

2013

AGRADECIMENTOS

Terminada mais uma etapa do meu percurso académico, gostaria de expressar a minha gratidão a todos os que de uma forma ou de outra contribuíram para o trabalho agora apresentado.

Primeiramente um muito obrigado à minha orientadora científica, a Doutora Ana Paula Silva, por me ter aceite no seu grupo, pelo que aprendi com a sua postura científica, espirito crítico, partilha de saber, correções e sugestões.

Ao Doutor Armando Cristovão, orientador interno desta dissertação, pela orientação científica, críticas construtivas e sugestões que muito contribuíram para a melhoria do trabalho realizado.

À Joana, ao Ricardo e á Vanessa pelo tempo disponibilizado na partilha de úteis conhecimentos e pela ajuda dada ao longo deste projecto.

À Fundação para a Ciência e Tecnologia (FCT), projeto PTDC/SAU-FCF/098685/2008 (fundos FEDER e COMPETE), cujo apoio foi determinante para a realização deste trabalho.

Last but not least… Á minha Família e Amigos. Apesar de não serem os primeiros nesta lista são certamente os primeiros no meu coração. Meu refúgio, meu apoio, meu lugar no mundo.

INDEX

ABBREVIATIONS

ACAMPs	Apoptotic cell associated molecular patterns
ADHD	Attention deficit hyperactivity disorder
AIF	Apoptosis-inducing factor
AJs	Adherens junctions
AMPA	α-amino-3-hydroxy-5-methyl-4-isoxazolepropionic acid
AMPT	α-methyl-p-tyrosine
ANOVA	Analysis of variance
ATCC	American Type Culture Collection
APC(s)	Antigen presenting cell(s)
ATP	Adenosine triphosphate
ATS	Amphetamine type stimulant
$A\beta_{1-42}$	Amyloid beta peptide 1-42
Bad	Bcl-2-associated death promotor protein
Bak	Bcl-2 homologous antagonist/killer protein
BL1, BL2	Basal lamina 1, basal lamina 2
Bax	Bcl-2-associated X protein
BBB	Blood-brain barrier
Bcl-X_L	B-cell lymphoma-extra large protein
Bcl-w	Bcl-2-like protein 2
Bcl-2	B-cell lymphoma 2 protein
Bid	BH3-interacting domain death agonist
BMVEC	Brain microvascular endotelial cells
BSA	Bovine serum albumin

Ca^{2+}	Calcium
$CaCl_2.2H_2O$	*Calcium chloride* dihydrate
CB	Cytochalasin B
CD	Cluster of differentiation
CM-H_2DCFDA	2',7'-dichlorodihydrofluorescein diacetate
CNS	Central nervous system
CO_2	Carbon dioxide
CuZn-SOD	Copper-zinc superoxide dismutase
DA	Dopamine
DAT	Dopamine transporter
DMEM	Dulbecco's Modified Eagle's Medium
DMSO	Dimethyl sulfoxide
DOPAC	3,4-Dihydroxyphenylacetic acid
ECM	Extracellular matrix
ECs	Endothelial cells
eNOS	endotheial nitric oxide synthase
ETC	Electron transport chain
FBS	Fetal bovine serum
FDA	Food and drug administration
GLU	Glutamate
GluR2	glutamate receptor 2
GLUT1	Glucose transporter 1
gp91	Glycoprotein 91
h	hour
H_2DCFDA	2',7'-dichlorodihydrofluorescein diacetate

H_2O	Dihydrogen monoxide
H_2O_2	Hydrogen peroxide
HAPI	Highly aggressively proliferating immortalized cells
hBEC	human brain endothelial cells
HCl	Hydrogen chloride
HEPES	4-(2-hydroxyethyl)-1-piperazineethanesulfonic acid
ICAM	Intercellular adhesion molecule-1
IDT	Instituto da Droga e Toxicodependência
IgSF	Immunoglobulin superfamily
Il-6	Interleucin-6
iNOS	inducible nitric oxide synthase
i.p.	Intraperitoneal
JAK 1, JAK2, JAK3	Janus Kinase 1, Janus kinase 2, Janus Kinase 3
JAK/STAT	Janus Kinase/Signal transducer and activator of transcription
JAMs	Junctional adhesion molecules
JNK	c-Jun N-terminal kinase
KCl	Potassium chloride
L-arg	L-arginine
L-NAME	L-NG-Nitroarginine Methyl Ester
LPS	Lipopolysaccharides
MAC	Macrophage antigen-1
MAO	Monoamine oxidase
METH	Methamphetamine
$MgCl_2.6H_2O$	Magnesium dichloride hexahydrate
MHC	Major histocompatibility complex

Min	minute
MMP(s)	Matrix metalloproteinase(s)
MMP-1, MMP-2, MMP-9	Matrix metalloproteinase 1, matrix metalloproteinase 2, matrix metalloproteinase 9
NFκB	Nucleas factor-κB
NMDA	N-methyl-D-aspartate
NMDAR	N-methyl-D-aspartate receptors
NR1	N-methyl-D-aspartate NR1 receptor
NR2A	N-methyl-D-aspartate NR2A receptor
NaCl	Sodium chloride
NADPH	Nicotinamide adenine dinucleotide phosphate
$NaNO_2$	Sodium nitrite
NO	Nitric oxide
nNOS	neuronal nitric oxide synthase
NOS	Nitrogen oxide synthase
NOS1, NOS2, NOS3	Nitric oxide synthase 1, nitric oxide synthase 2, nitric oxide synthase 3
NOX	NADPH-oxidase
O_2	Molecular oxygen
$O_2^{\cdot -}$	Superoxide anion
OH^-	Hydroxyl
ON	Overnight
$ONOO^-$	Peroxinitrite
OPC	Oligodendrocyte progenitor cells
OXPHOS	Oxidative phosphorylation

PAMPs	Pathogens-associated molecular patterns
PARP	Poly (ADP-ribose) polymerase
PBS	Phosphate-buffered saline
PIAS	Protein inhibitor of activated STAT
PRR(s)	Pattern recognition receptors(s)
PTPs	Protein tyrosine phosphatases
Rac2	Ras-related C3 botulinum toxin substrate 2
RNS	Reactive nitrogen species
ROS	Reactive oxygen species
RPMI	Roswell Park Memorial Institute medium
RT	Room Temperature
SEM	Standard error of the mean
SERT	Serotonin transporter
SHP1, SHP2	Src homology 1-containing tyrosine phosphatase, Src homology 2-containing tyrosine phosphatase
SOCS	Suppressor of cytokine signaling
SVZ	Subventricular zone
TCPTP	T-cell protein tyrosine phosphatase
TJ(s)	Tight junction(s)
TLR	Toll-like receptors
TNF	Tumor necrosis factor
TNF-α	Tumor necrosis factor alpha
TPH	Tryptophan hydroxylase
Tyk2	Tyrosine kinase 2
UNODC	United Nations Office on Drugs and Crime

VMAT	Vesicular monoamine transporter
ZO1, ZO2, ZO3	Zona occludens 1, zona occludens 2, zona occludens 3
3-NT	3-Nitrotyrosine
5-HT	5-Hydroxytryptamine terminals

RESUMO

A metanfetamina é uma droga de abuso altamente viciante e um potente estimulador do sistema nervoso central capaz de induzir danos em diferentes células e sistemas, como por exemplo o sistema dopaminérgico, serotoninérgico e glutamatérgico. De facto, a metanfetamina exerce inúmeros efeitos neurotóxicos entre os quais stresse oxidativo, excitotoxicidade e disfunção mitocondrial. Os níveis elevados de dopamina e glutamato levam à produção excessiva de espécies reactivas de nitrogénio e oxigénio. Recentemente, foi também sugerido que a metanfetamina compromete a integridade da barreira hematoencefálica. Esta barreira, ou mais especificamente a unidade neuronal-glial-vascular que é constituída por células endoteliais cerebrais, lâmina basal, neurónios, astrócitos, pericitos e microglia. Uma vez que a barreira hematoencefálica é uma estrutura complexa que providencia uma interface seletiva mas dinâmica entre a circulação periférica e o sistema nervoso central, alterações ao nível da sua função podem levar a lesões cerebrais. Quando a homeostase do cérebro é perturbada, ocorre uma reacção inflamatória envolvendo diversos tipos de células e moléculas, o que pode culminar com a morte celular. O processo neuroinflamatório envolve uma resposta complexa de todas as células do sistema nervoso central, incluindo neurónios, astrócitos, microglia e células endoteliais. Sabe-se que a metanfetamina é capaz de induzir neuroinflamação, contudo os seus efeitos específicos nas células da microglia e células endoteliais tem sido pouco estudado. Assim sendo, o objectivo do presente trabalho foi avaliar a resposta das células da microglia e endoteliais a um estímulo com metanfetamina, olhando especificamente para o stresse nitrosativo e oxidativo, usando duas linhas celulares como modelo de microglia e de células endoteliais, N9 e bEnd.3, respectivamente.

Neste estudo, observámos que a metanfetamina induz a libertação de nitritos em ambas as linhas celulares, 1 hora após a exposição a esta droga, tendo esta libertação sido prevenida na presença de L-NAME. Mostramos ainda que a via de sinalização JAK/STAT está envolvida neste efeito. Além disso, concluímos que a metanfetamina induziu um aumento dos níveis de 3-nitrotirosina. Apesar da rápida e transiente libertação de nitritos observada em ambas as linhas celulares, o aumento da produção de

espécies reactivas de oxigénio foi observada após 24 horas de exposição à droga, apenas em células da microglia. A viabilidade celular, após exposição à metanfetamina foi também avaliada em ambas as linhas celulares, sem nenhum efeito nas células da microglia. Contudo, uma diminuição da viabilidade das células endoteliais foi registada quando estas células foram expostas a concentrações elevadas de metanfetamina, o que pode ser uma possível explicação para a diminuição dos níveis de nitritos observada.

Com o presente estudo concluímos que a metanfetamina induz uma resposta nitrosativa em ambas as linhas células, enquanto o aumento das espécies reativas de oxigénio só foi observado nas células da microglia. Mais ainda, o efeito da metanfetamina parece ser dependente da concentração e tempo de exposição.

Palavras-chave: Metanfetamina, microglia, células endoteliais, óxido nítrico, 3-nitrotirosina, espécies reactivas de oxigénio.

ABSTRACT

Methamphetamine (METH) is a highly addictive drug of abuse and a potent central nervous system (CNS) stimulant able to induce damages to different cells and systems, such as dopaminergic, serotonergic and glutamatergic neurotransmission. METH-induced over-flow of dopamine and glutamate leads to excessive reactive nitrogen and oxygen species production. Indeed, this drug has several neurotoxic features that may include oxidative stress, excitotoxicity and mitochondrial dysfunction. Recently, it was also shown that METH compromises blood brain barrier (BBB) integrity. This barrier, or more specifically the neuro(glial)vascular unit, is composed by brain endothelial cells, basal lamina, neurons, astrocytes, pericytes and microglia. Since BBB is a complex structure that provides a restrict but dynamic interface between the peripheral circulation and the central nervous system (CNS), alterations in its function can lead to brain damage. When the homeostasis of the brain is disturbed, there is an inflammatory response involving several cells and molecules that can culminate in cell death. Neuroinflammatory process usually involves a complex response of all cells present within the CNS, including neurons, astrocytes, microglia and even endothelial cells. It is known that METH is able to induce a neuroinflammatory response, but the specific effect on microglial and endothelial cells have been overlooked. Thus, the present work focused on the study of METH-induced nitrosative and oxidative stress in both cell types, using as model two cell lines, N9 and bEnd.3**,** respectively for microglia and endothelial cells.

We observed that METH induces nitrites release by both cell lines at 1 h after drug exposure, which was prevented in the presence of L-NAME. Additionally, JAK/STAT pathway was shown to be involved in this effect. METH was also able to increase 3-nitrotyrosine (3-NT) levels. Despite of the quick and transient release of nitrites observed in both cell lines, the increase in the production of reactive oxygen species (ROS) was only observed at 24 h in microglial cells. Cell viability, was also evaluated in both cell lines, without an effect on microglial cells. However, we did observe a significant decrease in endothelial cell viability induced by high concentrations of METH, which can be one possible explanation for the decreased of nitrite levels observed.

Overall, we concluded that METH induces a nitrosative response in both microglial and endothelial cells, whereas the increase of ROS was only observed in microglial cells. Additionally, these effects were dependent on concentration and time exposure.

Keywords: Methamphetamine, microglial cells, endothelial cells, nitric oxide, 3-nitrotyrosine, reactive oxygen species.

Chapter 1 - Introduction

Chapter 1

Introduction

1.1 Methamphetamine

1.1.1 Methamphetamine consumption

Methamphetamine (N-methyl-O-phenylisopropylamine; METH) belongs to the group of amphetamine-type stimulants (ATS) (Davidson *et al.*, 2001; Berman *et al.*, 2008). All the substances included in this group share structural similarity with endogenous neurotransmitters, the monoamines [dopamine (DA), epinephrine (E), norepinephrine (NE) and serotonin (5-HT)], which confers them the similar biological actions and effects. METH structure consists of a phenyl ring connected to an amino group by a two-carbon side chain with a methyl group on carbon 1 of the side chain (Fig. 1.1) (Fleckenstein *et al.*, 2007). This drug is also known as speed, meth, chalk, ice, crystal or glass, and can be consumed orally, snorted, injected or smoked (National Institute of drug abuse).

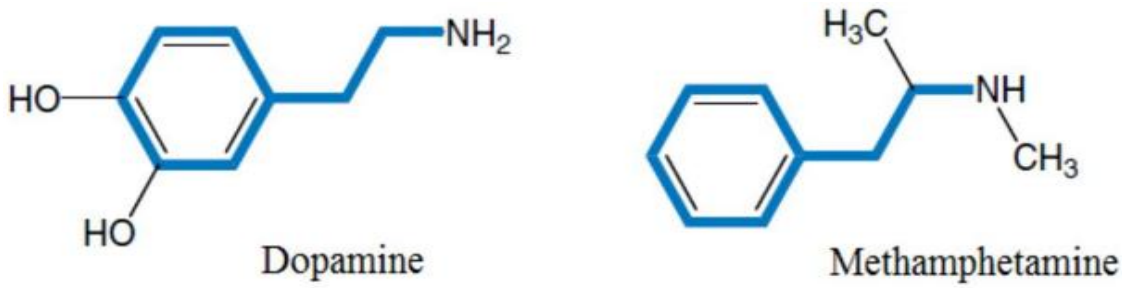

Figure 1.1 - Chemical structure of dopamine and methamphetamine showing their structural similarities (adapted from Fleckenstein *et al.*, 2007).

Despite being introduced in 1893, METH did not become widely used until World War II, when military personnel used it to combat fatigue and increase alertness (Meredith *et al*., 2005*)*. It was also prescribed in the 1950s and 1960s as a medication for depression, narcolepsy, attention deficit-hyperactivity disorder (ADHD), and obesity (Anglin *et al.*, 2000; Sulzer *et al.*, 2005; Berman *et al.*, 2008). Nowadays, METH is

approved by the Food and Drug Administration (FDA) for the treatment of ADHD, extreme obesity and narcolepsy (Sulzer *et al,*. 2005). Nevertheless, it is a controlled substance due to its probability to induce addition (Berman *et al.*, 2008). The great expansion of the METH market in the 1980s, made it one of the most wide-spread illicit drugs of abuse and has developed into an epidemic across the world (Rose and Grant, 2008). The increasing prevalence of illicit METH is in part due to its easy and low cost synthesis in clandestine laboratories. A number of different methods currently exist for synthesizing METH from legal precursor materials but the most popular, cheap, and simple method is the ephedrine/pseudoephedrine reduction.

Regarding METH consumption, data from the United Nations Office on Drugs and Crime (UNODC) World Drug Report 2012, ATS are the second most widely used class of drugs worldwide, with a number of 14.3 to 52.5 million users, aged 15-64, in 2010. In Portugal, according to the report from the *Instituto da droga e da toxicodependência*, IDT, (2011) between 2001 and 2007 there was an increase in amphetamines consumption from 0.5% to 0.9% in the total population, and from 0.6% to 1.3% in young population (Fig. 1.2).

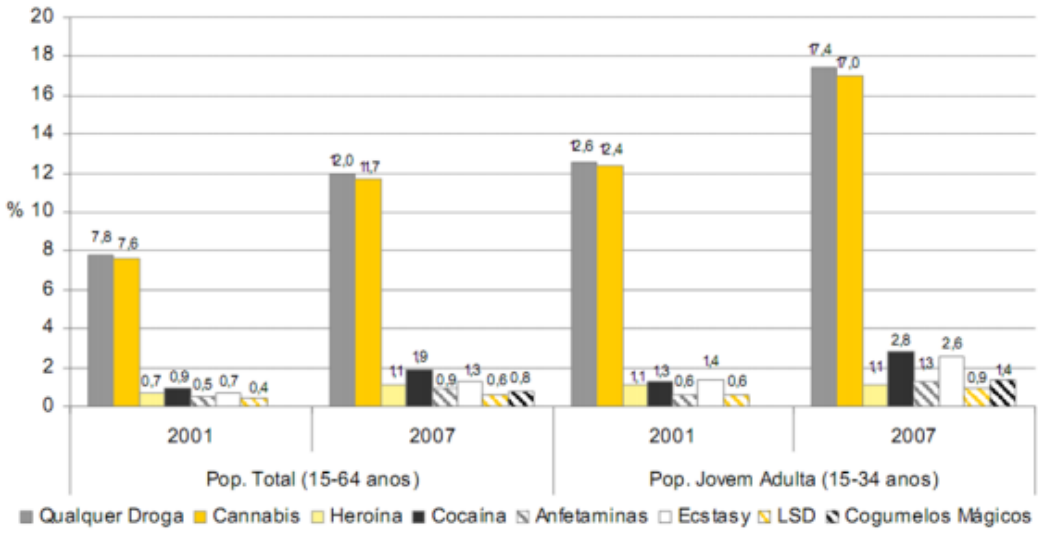

Figure 1.2 - Prevalence of different drugs consumption through life in total population and by young adults in Portugal (Annual Report of the Portuguese Institute for Drugs and Dependence, 2011).

1.1.2 Consequences of METH consumption

METH abusers can experience a large variety of effects depending if there is a chronic or acute consumption. Instants after consumption, users experience alertness, wakefulness, euphoria, increased activity (Quinton *et al*., 2006; Kish *et al.*, 2008), hyperthermia, and decrease in appetite (Yamamoto *et al*., 2010). Since METH has a relatively long half-life, about 12 hours (h), these pleasant effects can last for several hours (Derlet and Heischober, 1990). A chronic consumption has serious consequences such as renal and liver failure, life-threatening hyperthermia, cardiac arrhythmias, heart attacks, cerebrovascular hemorrhages, strokes, oral problems, seizures and death (Albertson *et al.*, 1999; Perez *et al.*, 1999; Donaldson and Goodchild, 2006; Darke *et al.*, 2008). Long-term use can also contribute to mood disturbances, confusion, anxiety, weight loss, insomnias, aggressiveness, social isolation and psychosis (Scott *et al*., 2007; Darke *et al.*, 2008; Homer *et al.*, 2008). Neuropsychological studies with human subjects demonstrate that METH chronic users have brain structural abnormalities, namely loss of gray matter, white matter hypertrophy and altered glucose metabolism in specific regions like hippocampus, prefrontal cortex, cingulated gyrus and amygdala (Thompson *et al.*, 2004; Berman *et al.*, 2008). In fact, these findings could explain some of the problems identified in METH users, such as behavioral alterations, recall capacity, memory and performance deficits observed on verbal memory tests and executive functions like problem solving (Thompson *et al.*, 2004). McCann and co-workers also made neuropsychiatric tests to abstinent METH users and demonstrated modest deficits in memory, «executive and motor function which are known to be modulated, in part, by the neurotransmitter DA (McCann *et al.*, 2008).

1.1.3 Cellular mechanisms of methamphetamine-induced neurotoxicity

1.1.1.1. Dopaminergic and serotonergic system dysfunction

The dopaminergic and serotonergic pathways are highly affected by METH due to the chemical structure similarity between METH and monoaminergic neurotransmitters. Under physiological conditions, neuronal activation promotes the release of DA into the synaptic cleft and when the stimulus is ceased, DA is removed by the DA transporter

(DAT) to the cytoplasm and by the vesicular monoamine transporter-2 (VMAT-2) into vesicles for storage, release and protection from oxidation. While DA is transported to the vesicle, H^+ is transported to the exterior of the vesicle, according to its concentration gradient. Such gradient is kept by an H^+-ATPase.

METH is able to diffuse through nerve terminals and consequently inducing the release of DA via the DAT-mediated reverse transport. Since METH shares structural similarity with DA (Fig 1.1), it can be also transported into the cell by DAT (Fig.1.3), leading to the release of DA according to its concentration gradient (Fleckenstein *et al.*, 2007). Moreover, METH can be transported by VMAT to the interior of the vesicle, accumulating in its interior, amphetamines are weak bases, therefore intravesicular METH accepts protons, leading to disruption of proton electrochemical gradient essential for the DA uptake, and then DA is accumulated in the cytoplasm. Moreover, METH is able to redistribute VMAT-2 (Hogan *et al.*, 2007) and to decrease the expression of dopamine transporters at the cell surface (by phosphorylation and internalization of the transporter) (Fleckenstein *et al.*, 2007). There is also evidence showing that METH interferes with enzymes involved in dopaminergic pathway. In fact, METH increases cytosolic levels of DA by inhibiting the activity of monoamine oxidase (MAO), as well as increases the activity and expression of the dopamine synthesizing enzyme, tyrosine hydroxylase (TH) (Barr *et al.*, 2006).

Although, the major reports have focused mainly on the effects of METH on the dopaminergic system, METH administration also induces toxicity to 5-hydroxytryptamine terminals (5-HT) (Quinton and Yamamoto, 2006). 5-HT and DA terminals are differently affected by METH, since it particularly affects DA terminals in the striatum (Wagner *et al.*, 1980; Ricaurte *et al.*, 1982), but 5-HT terminals are equally sensitive to the its toxic effects in various brain regions including hippocampus, prefrontal cortex, amygdala, and striatum (Ricaurte *et al.*, 1982; Seiden *et al.*, 1988). These effects in most DA markers (Wilson *et al.*, 1996; Volkow *et al*., 2001) and 5-HT transporter (SERT) (Sekine *et al.*, 2006) have also been observed in human chronic METH abusers by post-mortem analysis and imaging approaches. Ricaurte and McCann (1992) proposed that METH-induced DAT loss reflected irreversible terminal degeneration. However, studies in rodents (Friedman *et al.*, 1998; Cass and Manning, 1999), non-primates humans (Harvey *et al.*, 2000) and humans (Volkow *et al.*, 2001) have revealed significant recovery with protracted abstinence.

Studies have also emerged to show that DA plays an important role in the toxic effects of METH towards 5-HT axons. For example, α-methyl-p-tyrosine (AMPT), which was shown to protect against METH-induced toxicity towards DA axons, prevents long-term decrease in Tryptophan hydroxylase (TPH) activity and reductions in 5-HT levels in the striatum and hippocampus (Krasnova and Cadet, 2009).

1.1.1.2. Oxidative stress

METH neurotoxicity is characterized by the ability to prevent DA uptake into vesicles or to promote the accumulation of DA into the cytoplasm. DA can be metabolized into 3, 4-dihydroxyphenylacetic acid (DOPAC) and hydrogen peroxide (H_2O_2), or non-enzymatically auto-oxidized into cytotoxic DA-o-quinones or into DA semiquinones, with the production of reactive oxygen and nitrogen species non-enzymatically auto-oxidized into cytotoxic DA-o-quinones or into DA semiquinones, with the production of highly reactive superoxide anions (Fig. 1.3). These events lead to the production of reactive oxygen and nitrogen species (ROS and RNS, respectively), and lipid peroxidation (Fleckenstein *et al.*, 2007; Yamamoto *et al.*, 2010).

Diverse studies demonstrated the induction of oxidative stress by METH. For example, Gluck and collaborators (2001) used a repeated METH treatment [4x 10 mg/kg, each 2 h, intraperitoneal (i.p.)] showing that METH leads to the formation of lipid and protein markers of oxidative stress in mice striatum and hippocampus (Gluck *et al.,* 2001*)*. The role of oxidative stress is further supported by the findings that the neurotoxic effects of METH can be attenuated by free radical scavengers and antioxidants (Quinton and Yamamoto, 2006).

Furthermore, alterations in nitric oxide (NO) metabolism can also contribute to oxidative stress induced by METH (Itzhak and Ali, 2006). Wang and Angulo (2011) demonstrate an up-regulation of neuronal nitric oxide synthase (nNOS) and 3 nitrotyronine (3-NT) in mice striatum, using an acute METH administration (30 mg/kg, i.p.).

1.1.1.3. Glutamatergic system deregulation

Glutamate is the major excitatory neurotransmitter present in the mammalian central nervous system CNS. METH has been shown to increase the extracellular concentrations of glutamate (GLU) in the rat striatum (Nash and Yamamoto, 1992) and in the hippocampus (Rocher and Gardier, 2001). The increased extracellular GLU occurring during METH administration hyperactivates N-methyl-D-aspartate (NMDA) receptors (Fig.1.3), which increase intracellular Ca^{2+} that in turn activate enzymatic pathways leading to ROS and RNS production. Also, Ca^{2+} activates nitric oxide (NO) synthase with a consequent increased of NO levels (Fig.1.3) which can directly damage cells or react with superoxide to form highly reactive peroxynitrite ($ONOO^-$; Marshall and O´Dell, 2012). *In vitro* studies demonstrate that METH-induced cell death could be prevented by the inhibition of Ca^{2+} release from endoplasmatic reticulum (Smith *et al.*, 2010). Moreover, Simões and co-workers, observed that, in rat hippocampus, an acute METH administration (30 mg/kg, s.c.) increased glutamate receptor 2 (GluR2) and N-methyl-D-aspartate NR2A receptor (NR2A) protein levels without changes in N-methyl-D-aspartate NR1 receptor (NR1) subunit (Simões *et al.,* 2007). Although, striatal and cortical AMPA receptor subunit GluR2 protein levels were increased along with cortical NMDA receptor subunit NR1 down-regulation and NR2 up-regulation (Simões *et al.*2007).

1.1.1.4. Mitochondrial function impairment

The cationic lipophilic properties of METH confer the capacity to diffuse into mitochondria and be retained there, leading to matrix alkalinization (Sulzer and Rayport, 1990) and disruption of the mitochondrial membrane potential (Cunha-Oliveira *et al.*, 2006). More specifically, METH inhibits mitochondrial electron transport chain enzyme complex I (Klongpanichapak *et al.,* 2006), complex II-III (Brown *et al.*, 2005) and complex IV (Burrows *et al.*, 2000) with a consequent decrease of adenosine-5´-triphosphate (ATP) content in the brain and an increase of ROS production (Fig. 1.3) (Wu *et al.,* 2007). Furthermore, METH can alter mitochondria-dependent death pathway (Krasnova and Cadet, 2009). Jayanthi and co-workers showed that METH caused apoptotic cell death in frontal cortex of mice monoaminergic cells by increasing pro-apoptotic proteins, like Bax, Bad, Bak and Bid and decreasing anti-apoptotic proteins such as Bcl-2 and Bcl-X_L and Bclw

(Jayanthi *et al.*, 2001). METH also induced release of apoptosis-inducing factor (AIF), Smac/DIABLO and cytochrome c from mitochondria (Jayanthi *et al.*, 2004). Activation of caspase-3 upon METH administration has been reported in the rat frontal cortex (Warren *et al.*, 2007) and in rat cerebellar granule cells (Jiménez *et al.*, 2004). Several *in vitro* studies also point to apoptotic features induced by METH. For example, METH leads to early overexpression of Bax, decrease of mitochondrial cytochrome c and activation of caspase cascade (Deng *et al.*, 2002). More recently, Bento and co-workers, showed that METH triggered cell death of subventricular zone (SVZ) stem/progenitor cells by increasing caspase-3 activity (Bento *et al*.,2011*)*. These studies are corroborated by others pointing to protection of METH-induced cell death when caspases (Jimenez *et al.*, 2004) and PARP (Iwashita *et al.,* 2004) are inhibited, or when the anti-apoptotic Bcl-2 is up-regulated (Cadet *et al*., 1997).

1.1.1.5. Hyperthermia

Several studies demonstrate that hyperthermia is an important modulator of METH-induced toxicity to DA and 5-HT terminals. METH administration (4 x 10 mg/kg METH, i.p.) at room temperature produced a significant depletion of DA in the mice striatum, whereas equivalent doses of METH administered in a cold environment did not induce striatal DA and 5-HT depletions in the same brain region (Ali *et al*., 1994). It was also proposed that METH interacts with other mediators of METH toxicity such as GLU neurotransmission up-regulation and oxidative stress (Yamamoto *et al.*, 2010). In fact, the blockade of NMDA receptors provides a reduction of body temperature and protects against depletion of DA and 5-HT content and tyrosine hydroxylase (TH) activity in the mice striatum (Sonsala *et al.*, 1991; Bowyer, 1995). Furthermore, inhibition of METH-induced hyperthermia reduced ROS formation, which is able to attenuate DA toxicity in rat striatum (Fleckenstein *et al.*, 1997).

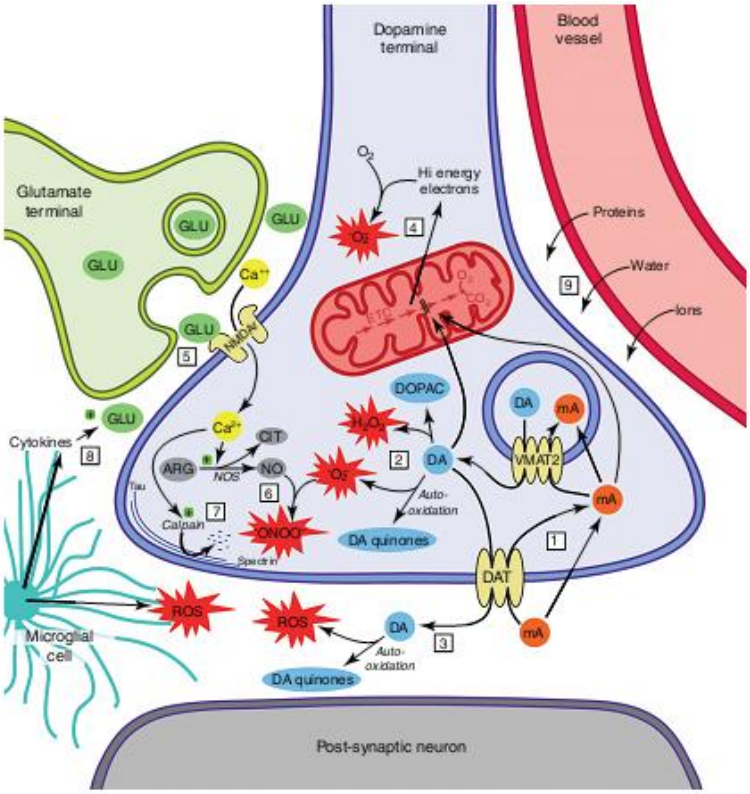

Figure 1.3 - Mechanisms of METH neurotoxicity. METH enters into dopaminergic terminals (1), causing efflux of DA from intraneuronal vesicles. This DA is oxidized intracellularly, producing reactive species (2) such as hydrogen peroxide (H_2O_2) and superoxide ($O_2^{\cdot-}$), and is transported to extracellular spaces (3) where it is also oxidized producing reactive oxygen species (ROS). High intracellular concentrations of DA and METH can inhibit the electron transport chain (ETC) in mitochondria (4), causing leakage of high-energy electrons which trigger the formation of superoxide. METH-induced an increase in GLU release (5), which hyperstimulates NMDA receptors (NMDAR) on dopaminergic terminals to cause increases in intracellular Ca^{2+}. Then, this Ca^{2+} will stimulates nitric oxide synthase (NOS) activity, increasing the production of nitric oxide (NO), which can combine with superoxide to form peroxynitrite ($^{\cdot}ONOO^{-}$) (6). METH also stimulates microglia to release ROS and cytokines (8) which increase extracellular GLU levels. Finally, METH causes leakage of the BBB, allowing plasma proteins to enter the brain (9) (Marshall and O'Dell, 2012).

1.2 Neuroinflammation

1.2.1 Innate and adaptative immune response

Brain innate immune response against an insult is based upon the activation of the resident glial cells (Hauwel *et al.*, 2005) and must be able to distinguish between *self* and *non-self molecules* (not expressed by host cells) designated pathogens-associated molecular patterns (PAMPS). Apoptotic cells also express specific molecules called apoptotic cell associated molecular patterns (ACAMPs). ACAMPs and PAMPs are further recognized by pattern recognition receptors (PRR) expressed at the surface of Toll-like receptors (TLRs; Gordon, 2002), the first element of contact between pathogens and the host (Akira *et al.*, 2001). Sometimes, interactions between TLRs and PAMPs fail to eliminate the infectious agent, leading to a response by glial cells and neurons, which begin with the production of inflammatory cytokines, chemokines and adhesion molecules. These factors will induce blood-brain barrier (BBB) disruption, allowing the entrance of adaptive immune components into the brain (Hisanaga *et al.*, 2001). Adaptive response starts with the antigen presentation of the stranger protein by antigen presenting cells (APC), complexed with surface major histocompatibility complex (MHC), to cluster of differentiation (CD)4^+ or $CD8^+$ T-cells, which became fully activated (Stone *et al.*, 2006). Immune response is further propagated by other T and B cells, recruited by activated $CD4^+$. Importantly, it was thought that BBB completely blocks the entrance of immune system cells into the brain parenchyma (Lucas *et al.*, 2006), but nowadays it is known that cells and molecules of the immune system can enter the brain (Nguyen *et al.*, 2002). Nevertheless, the flow of immune cells from the blood to the CNS, and vice-versa, is highly controlled by the endothelium (Huber *et al.*, 2001). Vascular endothelial cells are the target and source of inflammatory mediators (e.g. NO) and they have also a role in facilitating the passage of lymphocytes from blood to CNS through adhesion molecules, such as intercellular adhesion molecule-1 (ICAM-1) (Couraud, 1994; Wong, 1999).

1.2.2 Microglia

After an injury, immune system triggers an inflammatory response in order to restore homeostasis. The inflammation in the CNS, neuroinflammation, is a complex integration of the responses of all cells present within the CNS, including neurons, astrocytes, microglia and the infiltrating leukocytes (Carson *et al.*, 2006). Despite being able to produce pro-inflammatory cytokines (Park and Bowers, 2010), suppress T-cell activation (Tian *et al.*, 2009) and express class I MHC molecules (Ribic *et al.*, 2010), neurons are the most passive cells in the CNS immune response. On the other hand, microglia are the main responsible cells involved in innate immune response. These cells are derived from myeloid cells in the periphery and comprise approximately 12% of cells in the brain, being predominate in the grey matter, with the highest concentrations in the hippocampus, substantia nigra, basal ganglia and telencephalon (Block *et al.*, 2007). Under physiological conditions, microglia has a key role in monitoring the homeostasis of the brain, actively surveying the brain parenchyma for the presence of an insult (Kraft and Harry, 2011). Thus, an important feature of neuroinflammation is microglial activation, (Czeh *et al*., 2011) and the subsequent secretion of chemokines, cytokines and prostaglandins providing to the CNS a first line of response to the external insults (Lucas *et al.*, 2006; Farooqui *et al.*, 2007).

Microglia may present at least three phenotypic states: surveying ramified, activated non-phagocytic, and reactive, amoeboid phagocytic microglia (Figure 1.4). Under physiological conditions, microglia exhibit a resting ramified state, with a small cellular body. Despite being referred to as resting, microglia are constantly surveying the surrounding environment, being able to maintain homeostasis and identifying signals that require a response (Lull and Block, 2010). During this stage, microglia presents a surveying-like down-regulated immune phenotype, poor antigen presenting cells (APCs) with weak expression of MHC-II molecules, cytokines and their receptors, and no co-stimulatory molecules (Frei *et al.*, 1994). Occasionally, microglia is moderately activated to play the classic role as *scavengers* for the maintenance and restoration of the CNS. In response to brain insults, microglial cells are rapidly activated and their cell-surface receptor expression is modified, with up-regulation of surface receptors or antigen, such

as MHC-II and CD11b (Nakamura, 2002; Kim and de Vellis, 2005). Also, their phenotype is altered, cell body suffers swelling and became an amoeboid shaped cells with a phagocytic function. When activated, microglial cells are able to proliferate, migrate to the site of damage, and secrete pro- and anti-inflammatory cytokines, chemokines, stress inducing factors and growth factors (Hanisch and Kettenmann, 2007; Czeh *et al.*, 2011).

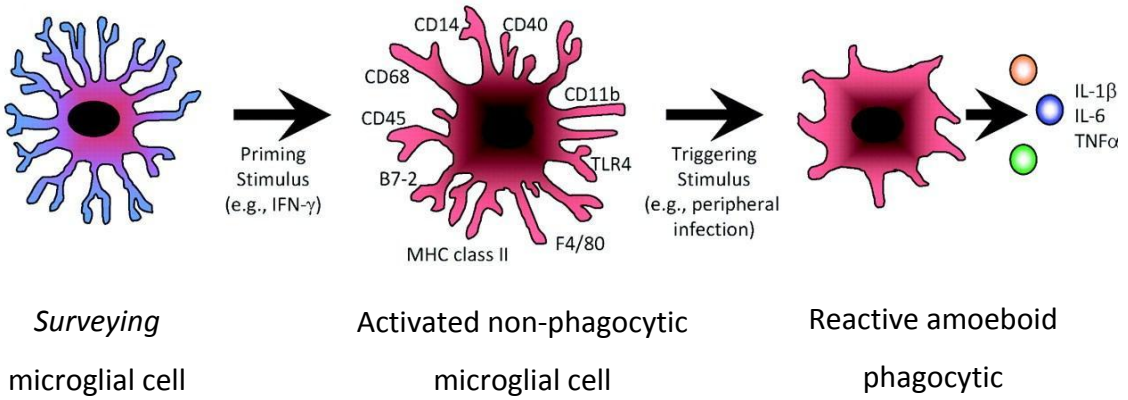

Figure 1.4 - **Morphological changes during microglial activation.** *Surveying* microglia is kept in stand-by mode to regulate CNS homeostasis. Several stimuli trigger microglia activation with antigen surface expression, proliferation, and migration. Transformed phagocytic microglia acquires the amoeboid shape and secretes various bioactive molecules, such as cytokines (adapted from Dilger and Johnson, 2008).

It is important to notice that microglial activation can be either beneficial or harmful, depending on the damage or stress exerted to the CNS (Walter and Neumann, 2009). Also, different pathways are activated when microglia are under a stress stimuli or during infection. Under bacterial invasion, a response called *classically activated microglia* (Fig. 1.5) is triggered. This response involves the expression of CD 86 and CD16/32, production of oxidative metabolites (NO, superoxide and hydrogen peroxide), pro-inflammatory cytokines and proteases (Hanisch and Kettenmann, 2007; Czeh *et al.*, 2011). As a consequence of this type of response, neuronal damage and reactive gliosis can be caused to healthy cells (Czeh *et al.*, 2011). Kacimi and collegues perform a study with co-cultures of endothelial and microglial cells, in which LPS-activated microglia promote BBB disruption through injury to endothelial cells, although in monocultures LPS induced microglial cell death but not endothelial cell (ECs) death (Kacimi *et al.*, 2011). In alternative, after a stress insult, microglia release anti-inflammatory factors and express

CD206 and arginase 1 leading to down-regulation of inflammation and tissue remodeling/repair (Fig. 1.5).

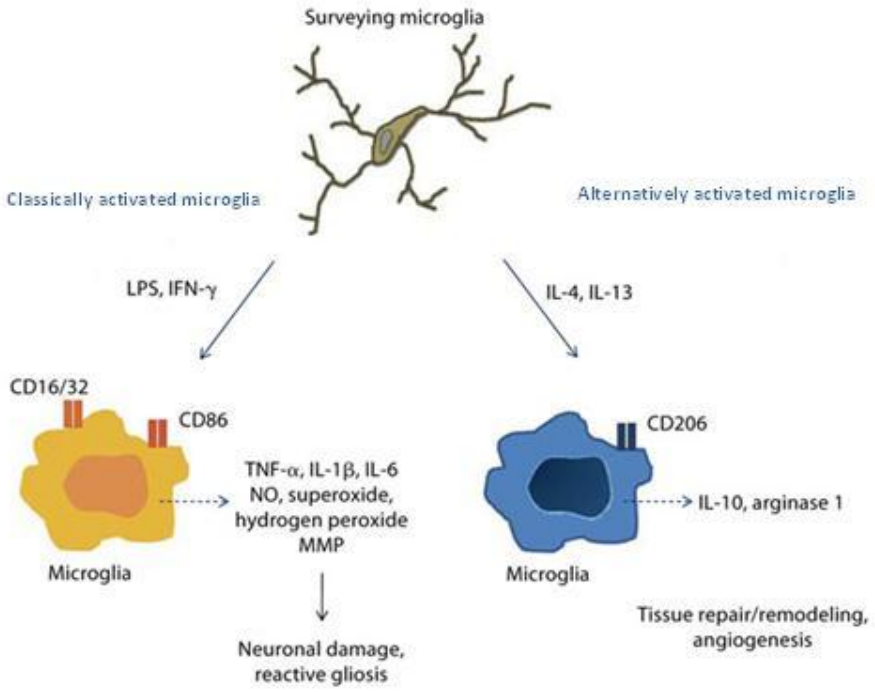

Figure 1.5 – Classical and alternative activated microglia. Microglial cells can be classified in a simplified manner into subsets of phenotypes and effector functions depending on the activation pathway (adapted from Czeh *et al.,* 2011).

Studies from our group, showed an acute high dose of METH (30 mg⁄kg, i.p.) triggers an inflammatory process characterized by microglia activation and increase of tumor necrosis factor (TNF) levels in the hippocampus, which was prevented by an anti-inflammatory treatment (Gonçalves *et al.*, 2010). More recently, using N9 cell line as an *in vitro* model, Coelho-Santos and colleagues demonstrated that METH induced microglial cell death and increase TNF-α and IL-6 extracellular and intracellular levels, as well as their receptor protein levels, at 1 h and 24 h post-exposure. Interestingly, exogenous low concentrations of TNF-α or IL-6 had a protective effect, suggesting a dual role for cytokines. Furthermore, the same study verified that activation of IL-6 signaling, specifically the JAK/STAT pathway, mediates the anti-apoptotic role of TNF-α, which in turn induced down-regulation of Bax/Bcl-2 ratio (Coelho-Santos *et al.*, 2012)

1.3 JAK/STAT signaling pathway

The Janus kinase/signal transducers and activators of transcription (JAK/STAT) pathway is one of a handful cascade used to transduce a multitude of signals for development (Kishimoto *et al.*, 1994). In mammals, the JAK/STAT pathway is the principal signaling pathway for a large variety of cytokine involved in immune response but also in the action of and growth factors and hormones and its activation stimulates cell proliferation, differentiation, cell migration and apoptosis (Huang *et al.*, 2008). Intracellular activation occurs when ligand binding induces the multimerization of receptor subunits. Depending on the ligand, the receptor subunits can be bound as homodimers or as heteromultimers, despite that, signal propagation through either homodimers or heteromultimers requires the association of cytoplasmic domains of two receptor subunits to JAK tyrosine kinases (Rawlings *et al.*, 2004). JAKs have kinase-homologous domains at the C-terminus, while the first is a non-catalytic regulatory domain, the second has tyrosine kinase activity. JAK family comprises four members: JAK1, JAK2, JAK3 and Tyrosine kinase 2 (Tyk2; Huang *et al.*, 2008) and its activation occurs upon ligand-mediated receptor multimerization because two JAKs are brought into close proximity, allowing trans-phosphorylation. The activated JAKs subsequently phosphorylate additional targets, including both the receptors and the major substrates, STATs witch are latent transcription factors that remain in the cytoplasm until activated. STATs have a conserved tyrosine residue near the C-terminus that is phosphorylated by JAKs (Shuai and Liu, 2003). This phosphotyrosine permits the dimerization of STATs through interaction with a conserved SH2 domain. Phosphorylated STATs enter the nucleus by a mechanism that is dependent on importin α-5 (also called nucleoprotein interactor 1) and the Ran nuclear import pathway (Heim, 1999). Once in the nucleus, dimerized STATs bind specific regulatory sequences to activate or repress transcription of target genes (Fig. 1.6); therefore, an initial extracellular signal is translated to a transcriptional response (Heim, 1999; Shuai and Liu*.,* 2003)

Some *in vitro* studies suggest the involvement of JAK/STAT pathway in microgial response. Kacimi and colleagues reported that inhibition of JAK/STAT improve microglial viability and reduce NO accumulation (Kacimi *et al.* 2011). Moreover, Coelho-Santos and

co-workers demonstrated the involvement of this signaling pathway in the prevention of METH-induced cell death by TNF-α and IL-6 (Coelho-Santos *et al.* 2012).

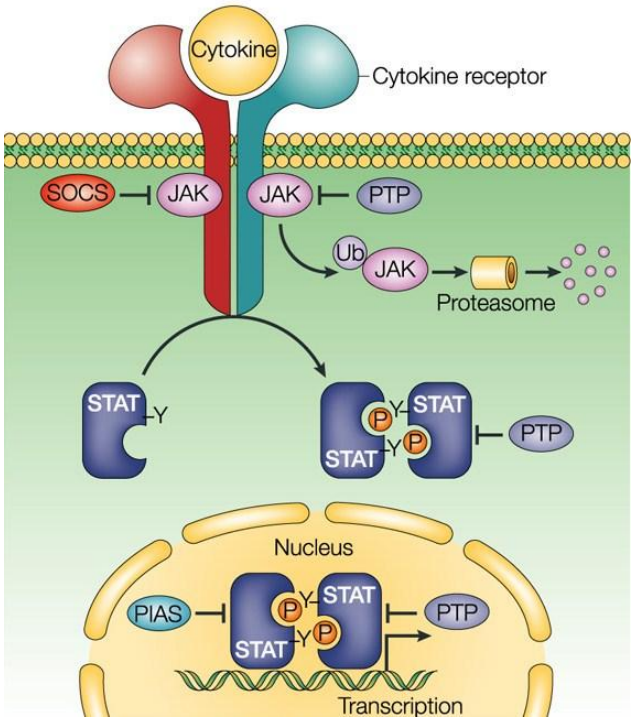

Figure 1.6 - Schematic representation of JAK/STAT signaling pathway. The Janus kinase (JAK)–signal transducer and activator of transcription (STAT) pathway is regulated at many levels. JAKs can be negatively regulated by suppressor of cytokine signalling (SOCS) proteins, protein tyrosine phosphatases (PTPs), such as SRC homology 2 (SH2)-domain-containing PTP1 (SHP1), SHP2, CD45 and T-cell PTP (TCPTP), and ubiquitin-mediated protein degradation. SOCS proteins, which are induced by cytokines, act as a negative-feedback loop to switch off the activity of JAKs. Many PTPs participate in the regulation of JAKs. The regulation of JAK2 by ubiquitylation (Ub) has also been suggested. The physiological significance of protein ubiquitylation in the regulation of JAKs remains to be determined. JAKs might also be regulated by other proteins, such as the SH2-B family of putative adaptor proteins (not shown). STATs can be negatively regulated by PTPs (such as PTP1B and TCPTP) in the cytoplasm, and by PIAS proteins, as well as PTPs (such as TCPTP and SHP2), in the nucleus. Protein inhibitor of activated STAT (PIAS) proteins interacts with STATs in response to cytokine stimulation and they inhibit the transcriptional activity of STATs through distinct mechanisms (Shuai and Liu., 2003).

1.4 Blood-brain barrier (BBB)

1.4.1 Functional Anatomy

Barrier layers at the key interfaces between neural tissue and blood play a major role in maintaining the homeostasis of the neural microenvironment (Sandoval and Witt, 2008). One of these barriers is the blood-brain barrier (BBB), which consists of an interdependent network of cells that separate the CNS from the systemic circulation. The barrier function is created at the level of the cerebral capillary endothelial cells (ECs)by tight junction formation. BBB acts as the gate-keeper of the CNS maintaining the fragile homeostasis of the brain (Abbott *et al.*, 2010) and is composed by a dynamic communication between neurons, microglia, astrocytes, pericytes, endothelial cells and extracellular-matrix (ECM), forming the neuro(glial)vascular unit (Fig. 1.7) (Hawkins and Davis, 2005). Brain endothelial cells , localized between blood and brain, play an important role in transport of micro and macronutrients, receptor-mediated signaling, leukocyte trafficking and osmoregulation (Persidsky *et al.*, 2006). ECs cytoplasm has uniform thickness with no fenestrae, low pinocytotic activity and continuous basement membrane (Boer and Gaillard, 2006). Another structural characteristic is the great number of mitochondria, providing energy for enzymes to break down compounds and allowing diverse selective transport systems to actively transport nutrients and other compounds into and out of the brain (Cardoso *et al.*, 2010).

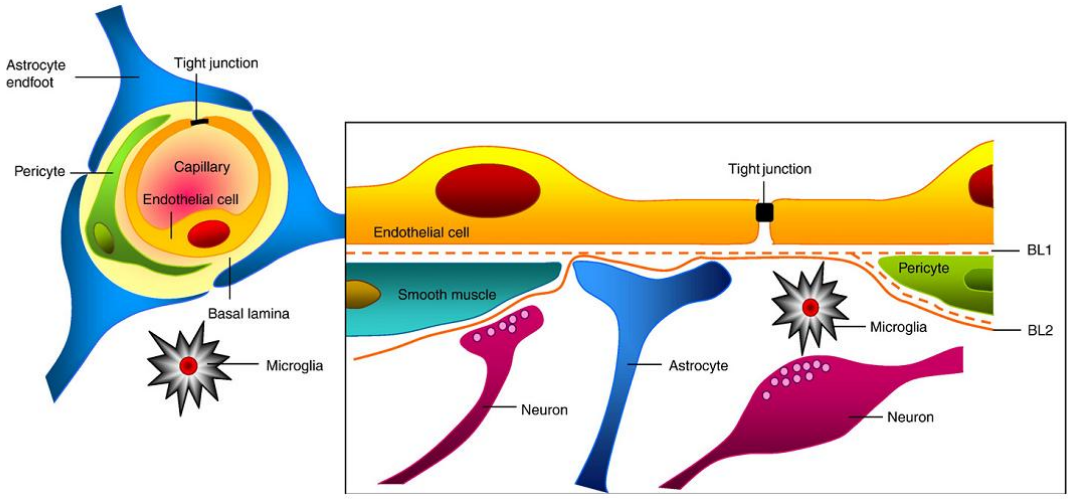

Figure 1.7 - Schematic representation of the neuro(glial)vascular unit. The cerebral endothelial cells have intercellular junctions that confer the barrier property of the BBB. Pericytes are distributed discontinously along the length of the cerebral capillaries. Both the cerebral endothelial cells and the pericytes are enclosed by, and contribute to, the local basement membrane which forms a distinct perivascular extracellular matrix (basal lamina 1, BL1), different in composition from the extracellular matrix of the glial endfeet bounding the brain parenchyma (BL2). Foot processes from astrocytes form a complex network surrounding the capillaries. Axonal projections from neurons contain vasoactive neurotransmitters that regulate local cerebral blood. Microglial cells have an immunovigilant function in the barrier (Abbott *et al.,* 2010).

BBB is characterized by the presence of an elaborated junctional complex that includes tight junction (TJ) and adherens junction (AJ) proteins. TJs include transmembrane proteins [claudins, occludin and junctional adhesion molecules molecules (JAMs)] and intracellular proteins such as zona occulens (ZO)-1, -2 and -3. ZO are accessory proteins linking TJ membrane proteins to the actin cytoskeleton (Hawkins and Davis, 2005). The AJs hold the cells together giving the tissue a structural support. Cadherin proteins cross the intercellular cleft and are linked into the cell cytoplasm by the scaffolding proteins α, β and γ catenin (Fig. 1.8). Both TJs and AJs are essential for barrier properties and alterations of these proteins may lead to BBB dysfunction (Persidsky *et al.*, 2006; Cecchelli *et al.*, 2007).

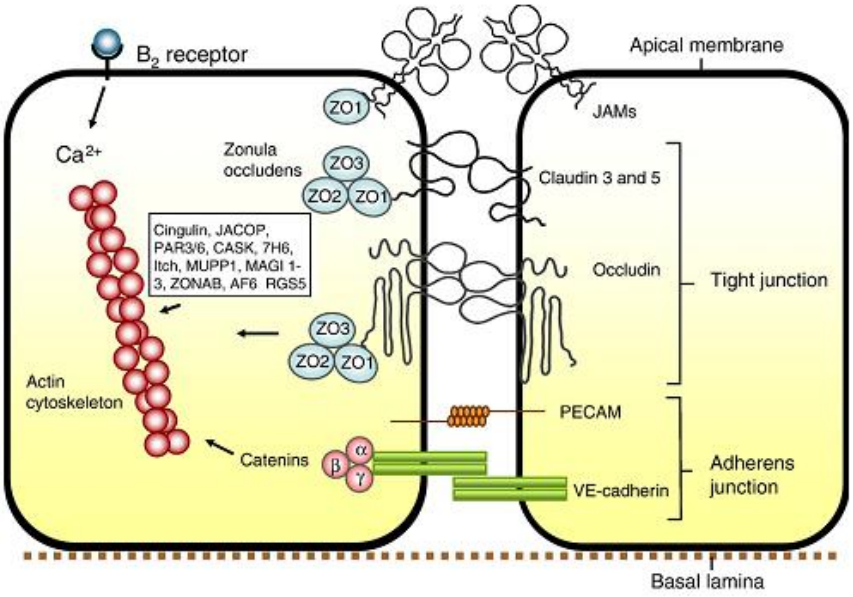

Figure 1.8 - Structure of BBB complex junctions. The tigh junctional complex comprises junctional adhesion molecules (JAMs), occludin and claudins. The claudins and occludin are linked to the scaffolding proteins ZO which in turn are linked *via* cingulin dimers to the actin/myosin cytoskeleton within the cell In the adherens junctions (AJs), VE-cadherin proteins are linked to the actin cytoskeleton by the scaffolding proteins catenin (Abbott *et al.*, 2010).

Despite the name *barrier*, BBB is a dynamic structure allowing the passage of several molecules *via* different routes of transport across the endothelial cells. The TJs confer to the BBB a highly impermeability to paracellular transport (Fig. 1.9a) through the junctions, forcing a transcellular route across the BBB (Abbott, 2006). Small gaseous molecules, such as molecular oxygen ($O_{2)}$ and carbon dioxide ($CO_{2)}$ can diffuse through lipid membranes, and this is also a route of entry for small lipophilic agents (Fig. 1.9b). The presence of specific transport systems on the luminal and abluminal membranes regulates the transcellular traffic of small hydrophilic molecules (Fig. 1.9c). Additionally, large molecules, such as peptides and proteins are transported by specific receptor-mediated transcytosis (Fig. 1.9d) or by the less specific adsorptive-mediated transcytosis (Fig. 1.9e) (Abbott *et al.*, 2006).

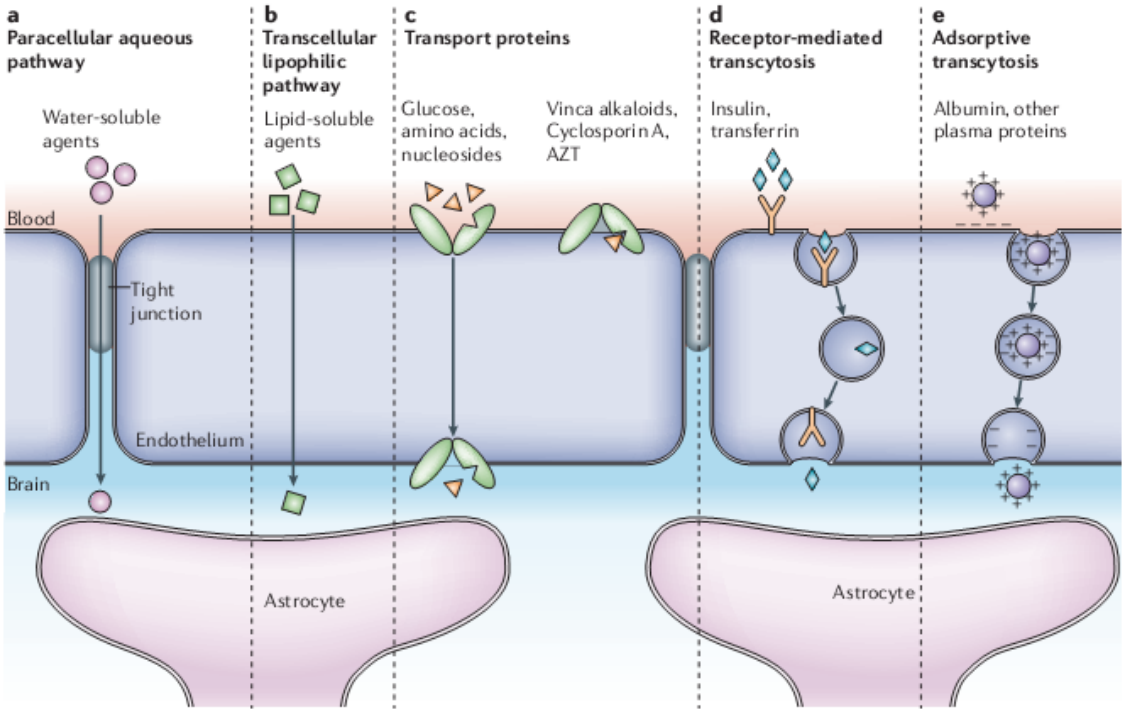

Figure 1.9 - Transport mechanisms at the blood-brain barrier. The paracellular transport is important for ionic homeostasis. The presence of specific transporters and transcytosis are essential to suppress the nutritional needs of the brain parenchyma. Nevertheless, transcytosis occur at a low level under physiological conditions (Abbott *et al.*, 2006).

1.4.2 Alterations of BBB function caused by METH

METH is a lipophilic molecule and a weak base, with low molecular weight and low protein binding capacity, allowing an easy diffusion across plasma membranes and lipid layers as BBB. After crossing BBB, METH activates an immediate signaling cascade that result in the release of monoamines (Martins *et al.,* 2011). However, METH has also a direct effect on BBB function. Recent studies have demonstrated the effects of METH on the BBB and a possible relationship to METH toxicity. In fact, it is already known that METH disrupts the BBB in several brain regions including the cortex, hippocampus, thalamus, hypothalamus, cerebellum, amygdala and striatum (Krasnova and Cadet, 2009). Specifically, Sharma and Kiyatkin showed increased BBB permeability using Evans blue and by leakage of serum albumin into the brain tissue in rats. An elevated brain temperature may also cause the breakdown of the BBB, resulting in brain edema, astrocytic activation and alterations of the CNS microenvironment (Sharma and Kiyatkin, 2009). Indeed, mild BBB dysfunction found in the caudate-putamen after METH

treatment was exacerbated by hyperthermia (Dietrich, 2009). Martins and colleagues also verified an increase in BBB permeability 24 h after administration of an acute high dose of METH, which was a transient effect since 72 h post-METH administration no leakage of Evans Blue was detected (Martins *et al.*, 2011).

In an attempt to understand the mechanisms responsible for METH-induced BBB dysfunction, Ramirez and colleagues demonstrated that METH compromises the barrier at the level of tight junctions. Microscopy analysis of immuno-fluorescence-labeled occludin and claudin-5 of primary brain endothelial cells (BMVEC) exposed to METH reveled low occludin and claudin-5 staining and gap formation (Ramirez *et al.,* 2009). Occludin, but not claudin-5, followed a time dependent decrease in expression (Ramirez *et al.*, 2009). Martins and colleagues confirm the previous results and also demonstrated a decrease in ZO-1 expression in the hippocampus, which can explain the increased BBB permeability. Furthermore, brain endothelial glucose transporter is also involved in BBB dysfunction (Martins *et al*. 2011). Recent data indicate that high concentration of METH decreased both the glucose uptake and glucose transporter 1 (GLUT1) protein levels in human brain endothelial cells (hBEC) culture. METH-induced decrease in GLUT1 protein level was associated with reduction in BBB tight junction protein occludin and ZO-1. Functional assessment of the trans-endothelial electrical resistance of the cell monolayers and permeability of dye tracers validate the pharmacokinetics and molecular findings that inhibition of glucose uptake by GLUT1 inhibitor cytochalasin B (CB) aggravated the METH-induced disruption of the BBB integrity (Muneer *et al.*, 2011).

Multiple studies suggest that METH-induced neurotoxicity involves oxidative stress (Yamamoto *et al.*, 2010). Ramirez and collaborators demonstrated that METH induced ROS in primary brain endothelial cells, decreased expression of TJ proteins and increased BBB permeability, although antioxidants prevented the production of oxidative radicals and restored monolayer integrity. The antioxidant Trolox prevented the increased permeability caused by METH (Ramirez *et al.*, 2009). Other key players are the metalloproteinases (MMPs) that can degrade tight junction proteins. In fact, METH increases the levels of MMP-9 and MMP-1, and amphetamine mediated oxidative stress is followed by activation of MMPs and breakdown of tight junction, which in turn leads to BBB disruption (Yamamoto *et al.*, 2010). Martins and colleagues, demonstrated an

increase in MMP-9 activity and immunoreactivity after 24 hours, at the hippocampus, correlated with decrease in TJ protein levels and BBB disruption. These results suggest that the increased activity and expression of MMP-9 is related with the decrease of claudin-5, occludin and ZO-1 expression and BBB disruption (Martins *et al.*, 2011). Furthermore, Urrutia and colleagues reported that inhibition of JNK pathway prevented METH-induced changes in MMP-9 activity, laminin degradation and BBB leakage (Urrutia *et al.*, 2013). Very recently, using brain microvascular endothelial cells (BMVECs), it was reported that NO is involved in METH-induced transcytosis (Martins *et al.*, 2013).

1.5 Role of inflammatory mediators in METH-induced brain dysfunction

1.5.1 Nitric oxide

NO, a small radical molecule, was identified in biological systems as an important intercellular gas messenger present in the cardiovascular, immune and nervous systems (Culotta, 1992). In brain, NO plays a dual action, being involved in physiological and pathological processes. It is implicated in the modulation of neuronal function such as synaptic plasticity (Prast and Philippu, 2001) and regulation of blood flow (MacMicking *et al.*, 1997). However, NO is also associated with neurodegenerative diseases and inflammation (Reis, 2006; Pacher *et al.,* 2007).

NO is produced *in vivo* by nitric oxide synthase (NOS), a highly regulated enzyme that uses L-arginine (L-arg) and O_2 as substrates (Palmer *et al.,* 1988).Garthwaite and collaborators demonstrated that activation of glutamatergic receptors, particularly the NMDA subtype, induces NO synthesis from L-arg in rat brain slices (Garthwaite *et al.,* 1988, 1989). This observation led to NOS cloning and isolation in the brain, where it was shown to be expressed by a number of different cells and regions (Bredt *et al.*, 1990, 1991; Schmidt *et al.*, 1991). Since this was the first NO synthase to be identified it was named NOS1 or neuronal NOS (nNOS), because it is typically expressed by neurons. Afterwards, a second isoform was isolated from macrophages and termed NOS2 or inducible NOS (iNOS; Hevel *et al.*, 1991; Stuehr *et al.*, 1991) because it could be readily induced by proinflammatory cytokines (Busse *et al.*, 1990; Radomski *et al.*, 1990) and is expressed in many cell types (such as endothelial and microglial cells). The first source of

NO identified, the endothelial NO synthase (NOS3 or eNOS) was the first to be identified but the last to be cloned and it is present in endothelial cells (Pollock *et al.*, 1991). These isoforms can also be divided according to their expression, being termed constitutive (nNOS and eNOS) because they are always present in a large cellular populations, or inducible (iNOS), as its expression depends largely on immunologic or inflammatory stimulus. Another major difference is that the latter is largely Ca^{2+}-independent (Busse *et al,.* 1990), whereas the former are not (Stuehr *et al.*, 1991). Importantly, iNOS gene has a STAT binding site in their promoter region (Kim *et al.*, 2008).

During the synthesis of NO by NOS, electrons from nicotinamide adenine dinucleotide phosphate (NADPH) flow between subunits to activate O_2 at the heme group, where L-arg is used to generate NO, L-citrulline and H_2O (Fig. 1.10, A). The enzyme converts the guanidino nitrogen of L-arg to NO and L-citrulline in a process that consumes five electrons (Bredt *et al.*, 1994) and requires it to cycle twice. In the first step, NOS consumes one mol of NADPH to hydroxylate L-arginine to Nω-hydroxyl-L-arginine, which is an enzyme-bound intermediate (Stuehr *et al.*, 1991). In an unusual second step, one electron from NADPH and another from Nω-hydroxyl-L-arginine lead to oxygen incorporation and scission of the C-N bond, yielding citrulline and NO (Fig. 1.10B; Stuehr *et al.,* 1991).

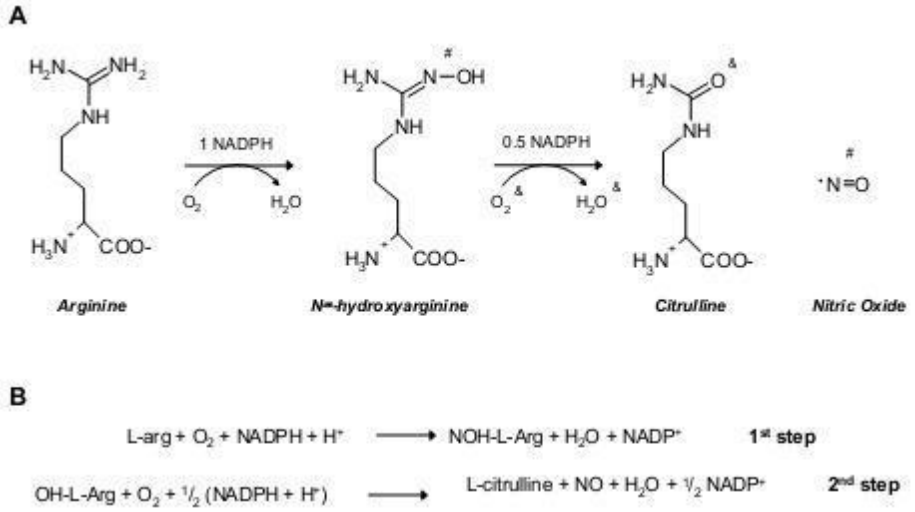

Figure 1.10 - Synthesis of NO by NOS. A) The guanidine nitrogen of L-arg is converted to NO in a two steps reaction at the heme group of NOS dimer. **B)** Partial reactions to form NO. Adapted from (Alderton *et al.*, 2001) and (Stuehr *et al.*, 2001).

NO can mediate a number of reactions by itself or it can also react with other molecules. We have shown that METH increased the activation of eNOS in rat endothelial cells, being involved in the transcytosis mediated by METH (Martins *et al.*, 2013). Additionally, there are several reports in the literature discussing the involvement of superoxide radicals ($O_2^{\cdot-}$) in METH-induced neurotoxicity (Cadet and Brannock*,* 1998). It has been reported that METH-induced dopaminergic depletion is attenuated in copper-zinc superoxide dismutase (CuZn-SOD) overexpressed transgenic mice (Cadet *et al.* 1995). Previously, we also referred that NO metabolism can contribute to oxidative stress induced by METH (Itzhak and Ali, 2006). Wang and Angulo demonstrated an up-regulation of neuronal nitric oxide synthase (nNOS) and 3-NT in mice striatum, using an acute METH administration (30 mg/kg, i.p.; Wang and Angulo, 2011). So, $O_2^{\cdot-}$ and NO interaction results in $ONOO^-$ formation, which plays a major role in METH-induced dopaminergic neurotoxicity. Because of its high reactivity under physiological conditions, direct measurement of $ONOO^-$ *in vivo* is not achieved easily. However, the nitration of tyrosyl residues has been shown to be a stable biochemical marker of $ONOO^-$ production both *in vitro* and *in vivo* (Beckamn *et al.*, 1994; Ischiropoulos, 1992). 3-NT results from the induction of nitration of tyrosine residues by $ONOO^-$, therefore 3-NT is a good indicator of peroxynitrite damage (Dijkstra *et al.*, 1998).

1.5.2 Reactive oxygen species

ROS are oxygen-containing molecules that react with and oxidize vulnerable cellular constituents, such as proteins, nucleic acids and lipids (Kraft and Harry, 2011). ROS are produced intracellularly through multiple mechanisms, mainly in the mitochondria, peroxisomes, endoplasmic reticulum, and the NADPH oxidase (NOX) complex in cell membranes (Muller, 2000). In eukaryotic cells the majority of energetic needs, ATP, is obtained by mitochondrial oxidative phosphorylation (OXPHOS), a process by which the oxidoreduction energy of mitochondrial electron transport is converted to the high-energy phosphate bond of ATP, which requires 4 supramolecular complexes of the respiratory chain and ATP-synthase. O_2 is the final electron acceptor for cytochrome-c oxidase (complex IV), the terminal enzymatic component of this mitochondrial enzymatic complex responsible for the four-electron reduction of O_2 to H_2O (Kocherginsky, 2009).

Partially reduced and highly reactive metabolites of O_2 may be formed during these (and other) electron transfer reactions. These O_2 metabolites include superoxide anion ($O_2^{\cdot-}$) and hydrogen peroxide (H_2O_2), formed by one- and two-electron reductions of O_2, respectively. When transition metal ions are present, the even more reactive hydroxyl radical ($OH^{\cdot}$) can be formed. These partially reduced metabolites of O_2 are often referred to as ROS due to their higher reactivity relative to molecular O_2 (Dikalov, 2011).

Microglia are a robust source of free radicals which can induce neuronal damage, and NADPH oxidase (membrane-bound enzyme that catalyses the production of superoxide from oxygen) is implicated as both the primary source of microglial-derived extracellular ROS and a mechanism of pro-inflammatory signalling in microglia (Babior, 1999). NADPH oxidase is activated by various stimuli, including bacterial PAMPs, inflammatory peptides and multiple neurotoxins. Several pattern recognition receptors (PRRs) activate NADPH oxidase, but the MAC1 receptor might be crucial for microglial NADPH oxidase activation in response to neurotoxic stimuli (Fig. 1.11). In resting cells, NADPH oxidase is composed of several subunits, and the cytosolic subunits (p47, p67, p40 and Rac2) are distributed between the cytosol and the membranes of intracellular vesicles and organelles (Babior*,* 1999). When microglia are activated, the cytosolic subunits translocate to membranes, where they bind to the membrane-associated subunits (p22 and gp91) and assemble the active oxidase to produce extracellular superoxide (Block *et al.,* 2007*).*

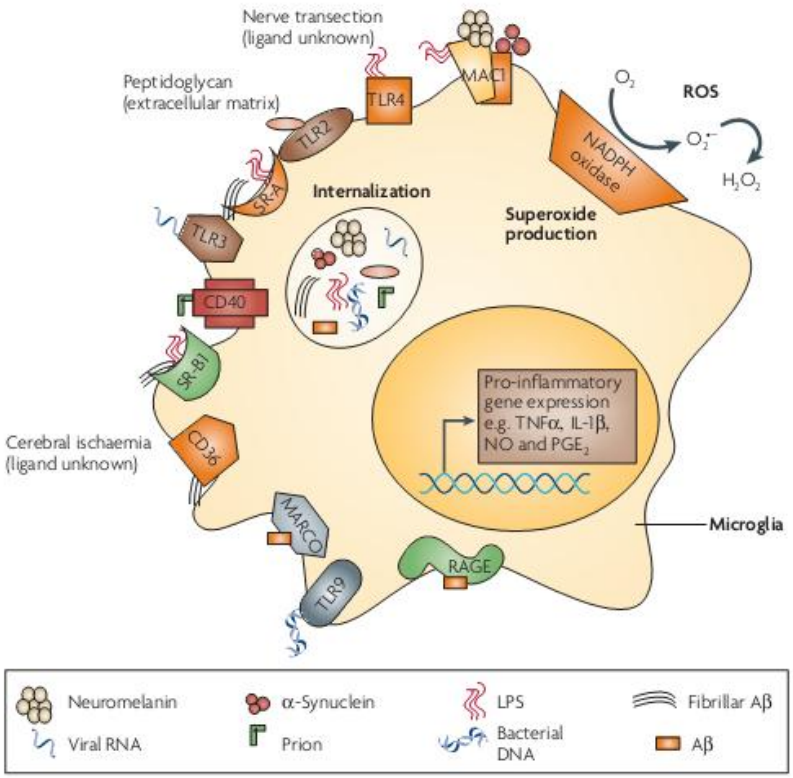

Figure 1.11 - Microglial PRRs identify neurotoxic and pro-inflammatory ligands. Microglia actively monitor the brain environment with pattern recognition receptors (PRRs). PRRs are responsible for several phagocytic functions such as the identification of pathogens, the production of extracellular superoxide, the release of pro-inflammatory compounds and the removal and destruction of toxic stimuli through internalization and phagocytosis (Block *et al.,* 2007)

1.6 Objectives

The impact of METH on the CNS has been extensively study, and the involvement of nitrosative and oxidative stress are some of the mechanisms responsible for METH-induced neurotoxicity. Nevertheless, many questions remain unanswered particularly regarding the direct effect of METH on microglial and endothelial cells. In fact, the majority of the hypotheses focused on neuronal events.

Therefore, the aim of the present work was to evaluate the inflammatory process triggered by METH on both microglial and endothelial cells, looking particularly for nitrosative and oxidative responses. For that, we performed a concentration- and time-dependent study to evaluate the alterations on nitrites, 3-nitrotyrosine and ROS levels. Cell viability was also analyzed.

Knowing that METH consumption is a serious worldwide health problem, and that induces brain dysfunction including neuropsychiatric disorders, it is crucial to understand its effect on the CNS.

Chapter 2 - Material and methods

Chapter 2

Material and methods

Cell culture

2.1.1 N9 cell line

The murine microglia cell line N9 (kindly provided by Prof. Claudia Verderio, CNR Institute of Neuroscience, Cellular and Molecular Pharmacology, Milan, Italy) was developed by immortalizing primary microglia cells with the v-myc or v-mil oncogenes of the avian retrovirus MH2 (Righi *et al.*, 1989). N9 microglial cells were cultured in RPMI (Gibco, Paisly, UK) supplemented with 5% fetal bovine serum (FBS; Gibco), 23.8 mM sodium bicarbonate (Sigma-Aldrich, St. Louis, MO, USA), 30 mM D-glucose (Sigma-Aldrich), 100 U/ml penicillin and 100 µg/ml streptomycin (Gibco). Cells were kept at 37^{o}C in a 95% atmospheric air and 5% CO_2 humidified incubator (Thermo Scientific Forma Series II, Marietta, USA) and grown in 75 cm^2 tissue flasks. Before plating cells for the different experimental procedures, the number of viable cells was evaluated by counting trypan-blue excluding cells with a hemocytometer cell counting chamber and plated at the densities indicated in Table I, according to the different experimental procedures.

Table I. Cell densities used to plate microglial cells according to the experiment.

Experiment	Nº cells/well	Multiwell culture plate	Medium volume	Final concentration
MTT assay	12000	96	150 µl	80000 cells/cm^2
Griess assay	40000	24	500 µl	80000 cells/cm^2
Immunocytochemistry	80000	12	1000 µl	80000 cells/cm^2
H_2DCFDA	12000	96	150 µl	80000 cells/cm^2

2.1.2 bEnd.3 cell line

The mouse brain endothelial cell line bEnd.3, originally generated in 1990 (Montesano *et al.*, 1990), was obtained from American Type Culture Collection (ATCC; Manassas, VA, USA). Cells were cultured in ATCC-formulated Dulbecco's Modified Eagle's Medium (DMEM; Gibco, UK) supplemented with 10% FBS (Gibco, Rockville, MD, USA), 100 U/ml penicillin, and 10 μg/ml streptomycin (Gibco). Cells were grown in 25 cm^2 tissue flasks and were maintained in a humidified cell culture incubator at 37^oC and 5% CO_2/95% atmospheric air. Before plating cells for the different experimental procedures, the number of viable cells was evaluated by counting trypan-blue excluding cells with a hemocytometer cell counting chamber. For all experiments cells were used in passage 26-34 and plated at the density of $2x10^4$cells/cm^2 and were allowed to reach confluence within 5-7 days and were used 3 days after reaching confluence. For all experiments, cells were in passage 26-34 and plated at a density of 2 x 10^4cells/cm^2.

2.2 Griess assay

Production of NO was determined through the formation and accumulation of its stable metabolite product, nitrite (NO_2^-), using a colorimetric assay, the Griess assay. According to the Griess reaction, under acidic conditions nitrite reacts with the amino group of sulfanilamide to form the diazonium cation, which couples to N-(1-naphthyl)ethylenediamine to form the corresponding red–violet coloured azo dye, with a maximum wavelength of 540 nm (Tsikas, 2007).

N9 cells were treated with METH [(+)-Methamphetamine hydrochloride, Sigma, USA; in μM: 1, 10 or 100] or 1 μg/ml LPS for 1, 4 and 24 h (Fig. 2.1), whereas bEnd.3 cells were treated with 250 μM, 1 mM, 3 mM METH or 1 μg/ml LPS for 1, 4 and 24 h (Fig. 2.2). Also, 1 mM L-NG-Nitroarginine methyl ester (L-NAME) was used as a pretreatment, during one hour, before incubation with 1 μM METH in N9 cells or 250 μM METH in bEnd.3 cells (Fig.2.1; Fig. 2.2). METH, LPS and L-NAME were diluted in Krebs solution [142 mM NaCl, 4 mM KCl, 1 mM $MgCl_2.6H_2O$, 1 mM $CaCl_2.2H_2O$, 10 mM Glucose, 10 mM HEPES (4-(2-hydroxyethyl)-1-piperazineethanesulfonic acid), pH 7.4]. Furthermore, to investigate if JAK/STAT pathway is involved in nitrite release induced by METH in N9 cells, we used 20

µM tyrphostin AG 490 (AG 490; Fig. 2.3), which inhibits the activation of STAT3 (Gorina *et al.*, 2007).

After treatments, 100 µl of supernatant was collected from wells and transferred to a 96-multiwell. Then, 100 µl of Griess reagent (1% sulfanilamide and 0.1% N-naphthylethyl-ethylenediamine dihy-drochloride in 5% phosphoric acid were mixed at a ratio of 1:1), was added to the calibration curve and samples. After 10 min of incubation, in the dark and at room temperature (RT), the nitrite released into the medium was quantified using a standard curve (performed in Krebs solution), obtained by serial dilutions of 4 mM sodium nitrite ($NaNO_2$; 0-200 µM). Absorbance was measured at 540 nm (reference 620 nm) on the Synergy™ HT multi-detection microplate reader (BioTek, Windoski, USA). The concentrations of sodium nitrite in control and exposed cells were plotted against the standard curve.

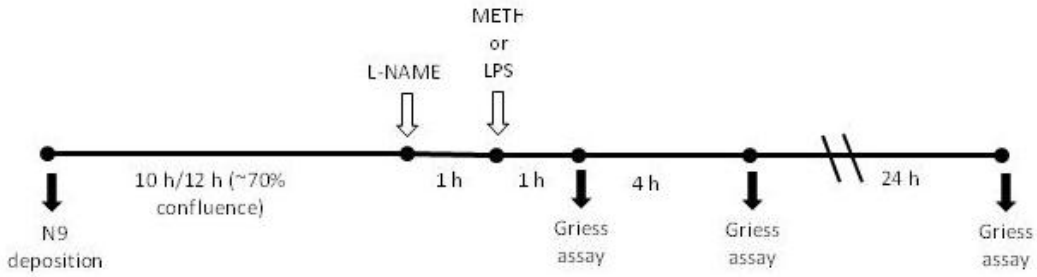

Figure 2.1 - Representation of the experimental design protocol used to investigate nitrite release in N9 cells. Cells were exposed to 1, 10, 100 µM METH or 1 µg/ml LPS during 1 h, 4 h or 24 h. Cells were also pre-treated during 1 h with 1 mM L-NAME and then co-exposed with 1 µM METH.

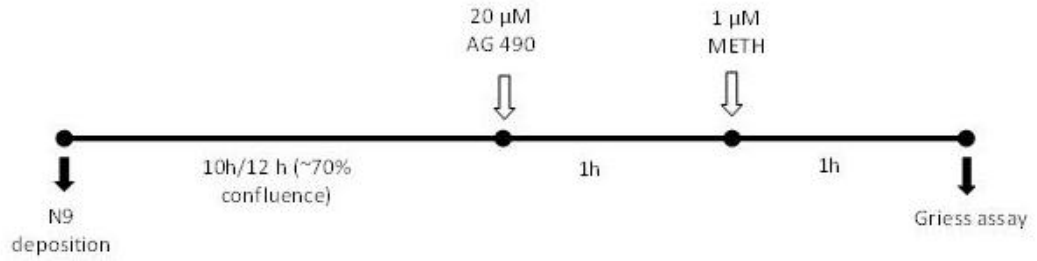

Figure 2.2 - Representation of the experimental design protocol used to investigate nitrite release in bEnd.3 cells. Cells were exposed to 250 µM, 1, 3 mM METH or 1 µg/ml LPS. Cells were also pre-treated during 1 h with 1 mM L-NAME and then co-exposed with 250 µM METH.

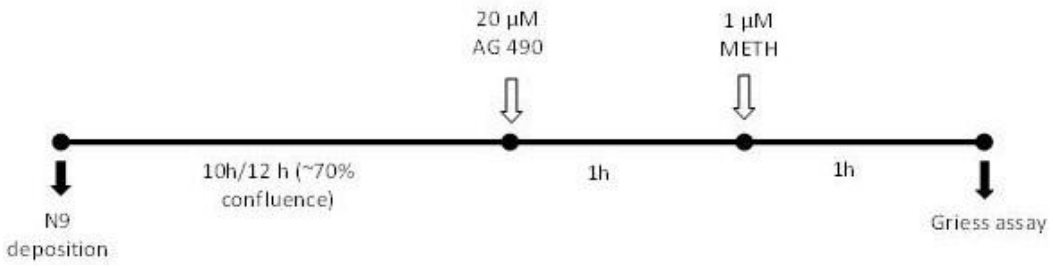

Figure 2.3 - Representation of the experimental design protocol used to investigate JAK/STAT pathway involvement in nitrite release by N9 cells. Cells were exposed to 1 µM METH. Cells were also pre-treated during 1 h with 20 µM AG490 and then co-exposed with 1 µM METH.

2.3 MTT assay

The reduction of 3-(4,5-dimethylthiazol-2-yl)-2,5-diphenyl-tetrazolium bromide (MTT, yellow colored) to tetrazole was used to evaluate cell viability. This is a colorimetric assay in which MTT is reduced by metabolically active cells to insoluble purple formazan dye crystals. The rate of tetrazolium reduction is proportional to the rate of mitochondrial enzyme succinate dehydrogenase activity (Mosmann, 1983).

N9 cells were plated in 96-wells culture plates, allowed to grow until reach confluence and then incubated with METH for 1, 4 and 24 h.

The bEnd.3 cells were seeded on a 96–multiwell plate and were allowed to grown until reach confluence and then incubated with a concentration of 1 or 3 mM METH for 1, 4 and 24 h.

After treatments, the medium was removed and the cells were washed with Krebs solution and 0.5 mg/ml MTT solution was added to each well and cells were kept at 37^{o}C in a 95% atmospheric air and 5% CO_2 humidified incubator (Thermo Scientific Forma Series II) for 3 hours. The crystals were then dissolved in dimethyl sulfoxide (DMSO) with vigorous resuspension. The resulting purple needle-shaped crystals were dissolved by the addition of acidic isopropanol (0.04 M HCl in absolute isopropanol). To completely solubilize the crystals, repetitive pipetting was applied and the plate was stirred on an automatic plate shaker in the dark at RT. Absorbance was measured at 570 nm (reference 620 nm) on the Synergy^{TM} HT multi-detection microplate reader (BioTek).

2.4 Immunocytochemistry

Double-labeling immunofluorescence was performed for 3-NT and a microglial marker, CD11b. Briefly, cells were exposed to 1 µM METH for 1 h or pretreated during 1 h with 1 mM L-NAME and then co-exposed with 1 µM METH for one more hour (Fig. 2.4). A positive control was also performed exposing cells to 10 mM $NaNO_2$. After treatments, cells were rinsed with PBS, fixed with ethanol:acetic acid [95:5] for one minute at RT, washed with PBS and blocked with a solution of 1% BSA in PBS for 30 min. Afterwards, cells were incubated with rabbit anti-mouse 3-NT antibody (1:100; Millipore, Billerica, MA, USA), in PBS with 1% BSA, 4^0C overnight (ON). After washed, cells were incubated with the secondary antibody Alexa Fluor 488 (1:200; Invitrogen, Inchinnan Business Park, UK) for 1 h 30 min at RT and from this point forward cells were protected from light. Cells were again washed and blocked with 1% BSA in PBS for 30 min, and incubated with rat anti-mouse CD11b antibody (1:500; AbD Serotec, Oxford, UK) for 3 h at RT. After the incubation, cells were washed one more time and incubated with Alexa Fluor 594 (1:200; Invitrogen) for 1 h 30 min RT. The cells were then washed and stained with 4 µg/ml Hoechst 33342 for 5 min at RT in the dark. Finally, cells were washed and mounted in DakoCytomation fluorescent medium and stored in dark at 4^oC until examined in a LSM 710 Meta confocal microscope (Carl Zeiss, Göttingen, Germany).

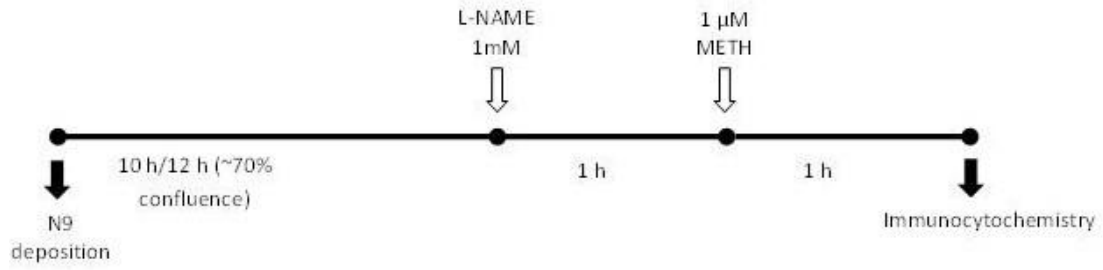

Figure 2.4 - Representation of the experimental design protocol used to investigate 3-NT immunoreactivity in N9 cells. Cells were exposed to 1 µM METH and also pre-treated during 1 h with 1 µM L-NAME and then co-exposed with 1 µM METH.

2.5 Detection of intracellular levels of reactive oxygen species (ROS)

Intracellular levels of ROS can be detected by fluorimetry, using dichlorofluorescein (H_2DCFDA) probe. H_2DCFDA is able to cross the cell membrane and their acetate groups are removed by intracellular esterases, producing H_2DCF. H_2DCF reacts with several cytotoxic oxygen species producing 2',7'-dichlorofluorescein (DCF) that can be used as a measure of intracellular ROS levels (NEVŘELOVÁ *et al.*, 2005).

Microglial cells were plated on black 96-multiwells, and METH (1, 10 and 100 µM) or 1 µg/ml LPS were added for 1, 4 and 24 h. bEnd.3 cells were also plated on black 96-multiwells and after reaching confluence, cells were exposed to METH (250 µM, 1 and 3 mM) or 1 µg/ml LPS for 1, 4 and 24 h. Immediately after treatments, medium was removed and cells were incubated with 5 µM H_2DCFDA diluted in PBS (in dark conditions) and kept at 37^{o}C in a 95% atmospheric air and 5% CO_2 humidified incubator (Thermo Scientific Forma Series II, Marietta, USA). The excitation and emission filters used for the H_2DCFDA probe were 485/20 nm and 528/35 nm respectively. The value after bar indicates slip values used.

2.6 Statistical analysis

Statistical analysis was performed using GraphPad Prism 5.0 (GraphPad Software, San Diego, CA). Statistical significance was considered relevant for $P<0.05$ using one-way analysis of variance followed by Dunnett´s post hoc test for comparison with control condition, followed by Bonferroni´s post hoc test for comparison among experimental conditions. In MTT studies performed with b.End3 cell line, statistical significance was determined using two-tailed student t-test. Data were presented as mean±SEM (standard error of the mean). To normalize results between experiments, the results of each experiment were expressed as the percentage of control.

Chapter 3 - Results

Chapter 3

Results

3.1 Methamphetamine-induced production of nitrites by microglial and endothelial cells

Microglial activation, a crucial feature of the inflammatory response in the CNS, is characterized by the release of inflammatory mediators such as cytokines, NO and prostaglandins (Huo *et al.,* 2011; Kamici *et al.*, 2011). Regarding drugs of abuse, Sekine and colleagues demonstrated microglial activation in human brain of METH abusers (Sekine *et al.*, 2008), furthermore results from our group also showed that METH triggers a microglial response in the mice hipoccampus (Gonçalves *et al*., 2010).

In the present study, we aimed to evaluate if METH induces the release of nitrites by microglial cells. For that, we used the N9 cell line and the griess assay. Cells were exposed to METH (1, 10 or 100 µM) during 1, 4 or 24 h. LPS (1 µg/ml), synthesized by gram negative bacteria, was used as an inflammatory insult since it is a complex macromolecule containing a polysaccharide group covalently linked to a unique lipid structure (Block *et al.*, 2007). In fact, LPS is widely used to activate several inflammatory signaling cascades, including the secretion of proinflammatory cytokines by microglial cells (Burguillos *et al.*, 2011). Here, we observed that 1 h after 1 µM METH administration (Fig. 1A) there was a significant release of nitrites (180.83+10.90% of control; ***P<0.001, n=24), which was completely abolished in the presence of 1 mM L-NAME (1 mM L-NAME + 1 µM METH: 93.08±8.90% of control, +++ P<0.001, n=18), a non-selective NOS inhibitor. Additionally, 1 µg/ml LPS also triggered the release of nitrites (151.19±9.17% of control, **P<0.01, n=10) when compared to the control (100.0±6.48%, n=13). Higher concentrations of METH or L-NAME did not lead to differences when compared to the control (10 µM METH: 101.28±6.17% of control; n=18; 100 µM: 96.84±12.35% of control, n=7; L-NAME: 98.65±5.56% of control, n=27). Furthermore, after 4h (Fig. 1B) or 24 h (Fig. 1C) we did not observe any significant differences when compared to the control, after METH treatment, showing that METH triggers a response of microglial cells within 1h and then returning to basal conditions. However, LPS induced a significant increase in nitrites

levels at 24 h (158.59±10.05, **P<0.01, n=5) and a tendency to increase nitrite levels, although not significant, at 4 h (121.56±1.94, n=6). Importantly, all the METH concentrations used did not induced cell death (Coelho-Santos *et al.*, 2012).

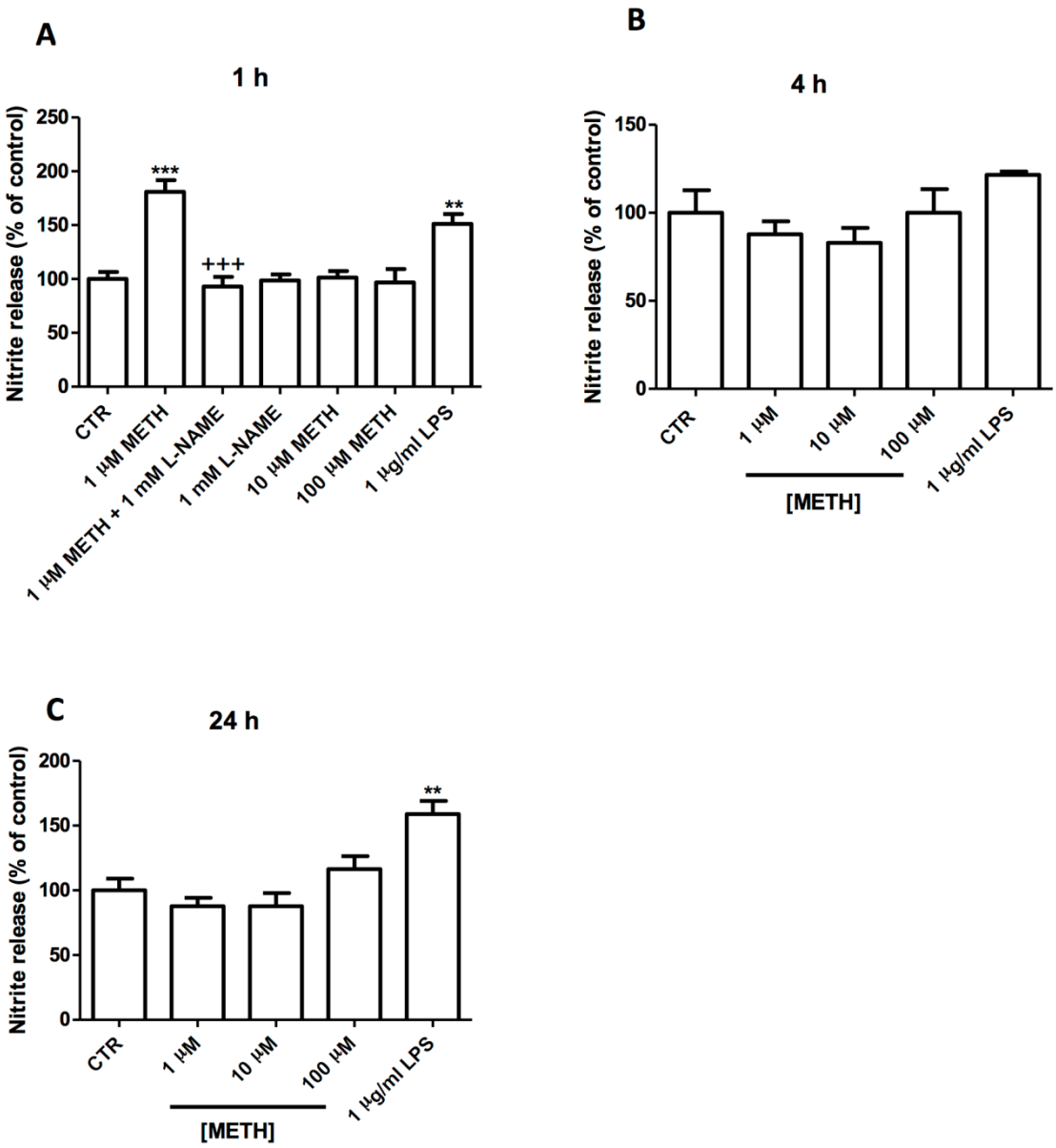

Figure 3.1 - Release of nitrites in N9 cell line after **(A)** 1 h, **(B)** 4h or **(C)** 24h of METH exposure. The results are expressed as mean percentage of control (±SEM) n=4-27. **P<0.01; ***P<0.001, significantly different from control using Dunnett´s post-test. +++P<0.001, significantly different from 1 µM METH using Bonferroni´s post-test.

Recent studies showed that an up-regulation of nitrate lead to the accumulation of 3-nitrotyrosine (3-NT) in mice striatum (Wang and Angulo, 2011). Moreover, in the

present work, we demonstrated an increase in nitrite levels at 1h after 1 µM METH exposure (Fig. 3.1A). Thus, we also performed immunocytochemistry studies to corroborate our results. In fact, we were able to clearly show an increase in 3-NT immunoreactivity and as a positive control we used 10 mM sodium nitrite (Fig. 3.2).

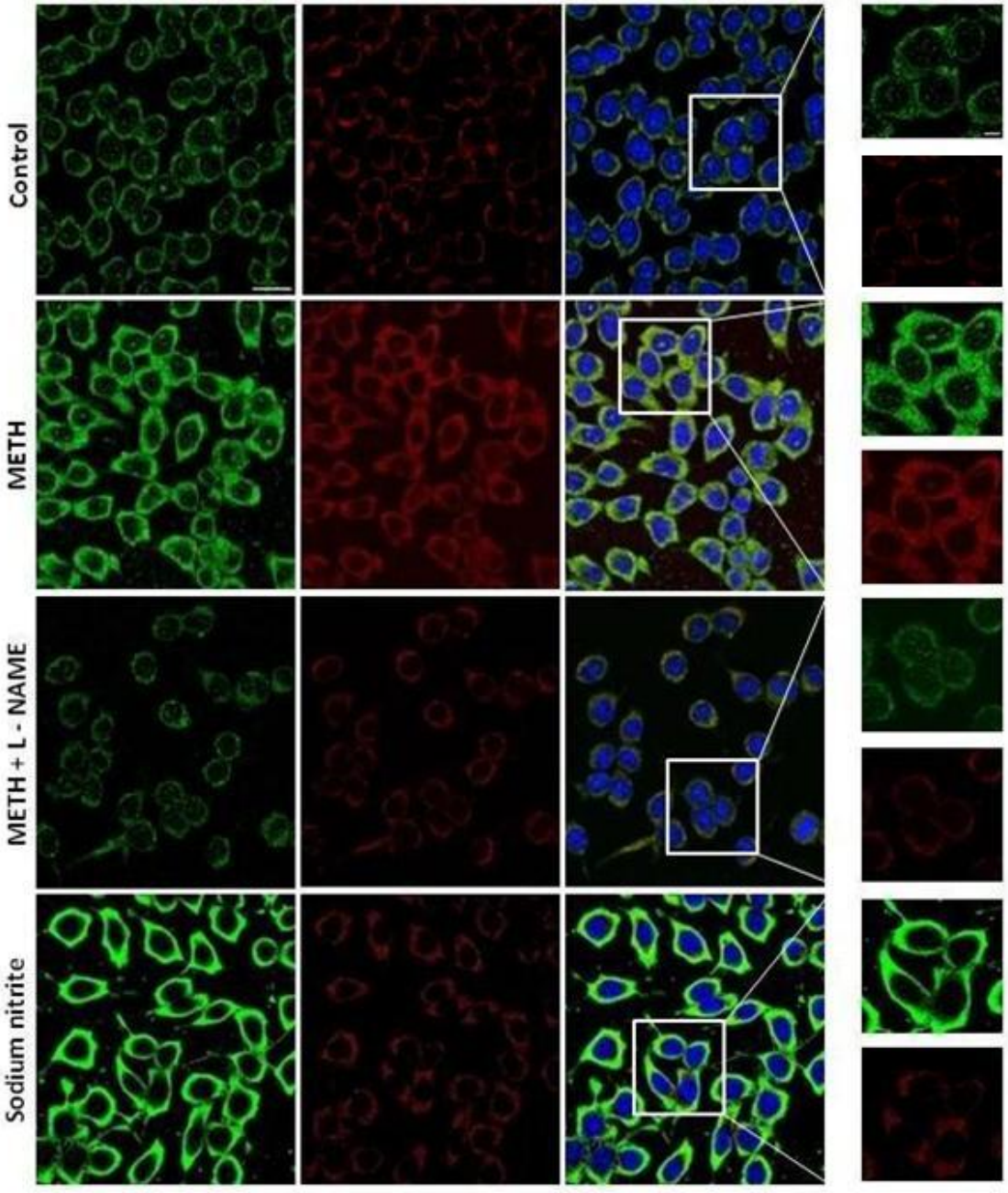

Figure 3.2 - METH increases 3-nitrotyrosine expression. Representative confocal images of 3-NT (green) and CD11b (red) immunoreactivity in N9 microglial cells under control conditions, exposure to 1 µM METH, 1 µM METH pretreated with 1 mM L-NAME or to 10 mM sodium nitrite. Cells were stained with Hoechest 3342 (blue). Scale bar 20 µm or 5 µm (crop).

JAK-STAT cascade is an essential inflammatory signaling pathway that mediates immune and inflammatory response (Park *et al.*, 2003; Dziennis and Alkayed, 2008). Binding of ligands to its receptors induces the phosphorylation of receptor-associated JAK, which in turn leads to STAT phosphorylation. After phosphorylation, STAT forms dimers and translocates into the nucleus to regulate the transcription of target genes encoding proinflammatory cytokines, chemokines and inducible enzymes such as iNOS and Cox-2 (Ganster *et al.*, 2001; Kovarik *et al.*, 2001). AG 490 belongs to the tyrphostin family of tyrosine kinase inhibitors and has been used to selectively block the JAK/STAT3 signaling pathway and to inhibit the activation of STAT3 in microglia cells (Kim *et al.*, 2002; Zhu *et al.*, 2008).

Prompted by these findings, we use AG 490, a JAK-STAT inhibitor to further identify underlying mechanisms involved in nitrites release induced by METH in microglial cells. Here, cells were pre-treated during 1 h with 20 µM AG 490 and then co-exposed with 1 µM METH for 1 h. We observed that AG 490 blocked the increase in nitrite release induced by METH, when compared with METH alone (117.23±18.83% of control, ++ P<0.01, n=7) indicating that activation of JAK-STAT pathway is involved in increased levels of nitrite release induced by METH (Fig.3.3).

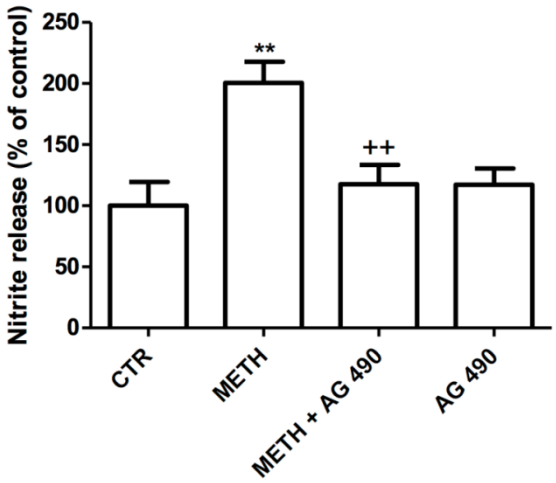

Figure 3.3 - JAK/STAT inhibition blocked nitrite release triggered by 1 µM METH in N9 cell line. The results are expressed as mean percentage of control (±SEM) n=3-9. **P<0.01, significantly different from control using Dunnett´s post-test. ++P<0.01, significantly different from 1 µM METH using Bonferroni´s post-test.

It is already well established that METH induces BBB dysfunction (Mahajan *et al*., 2008; Ramirez *et al.*, 2009; Martins *et al.*, 2011; Urrutia *et al.*, 2013.). Additionally, among the features of METH toxicity there is the production of RNS such as NO (Quinton and Yamamoto, 2006), and it has already been implicated in increased BBB permeability. Yamagata and co-workers related NO-mediated increased permeability with changes in the expression of TJ proteins and a redistribution of AJ proteins, pointing to a role of NO in signal transduction cascades induced by hypoxia that leads to junctional disorganization and BBB breakdown (Yamamoto, *et al.*2004). Taking this information into account, we further aimed to clarify if METH also triggers the release of nitrites by endothelial cells, using for that the bEnd.3 cell line. Griess assay was performed at 1, 4 and 24 h post-METH, and results showed that at 1 h there was a significant decrease of nitrites induced by 3 mM METH (48.03±3.67% of control, ***P<0.001, n=9; Fig. 3.4A). Nevertheless, in the presence of 250 µM METH there was a significant increase in the release of nitrites (130.70± 5.01% of control, *P<0.05, n= 14) which was significantly prevented by L-NAME pretreatment (METH + L-NAME: 87.23±6.18% of control, ***P<0,001 n=13).

Furthermore, 4 h after METH treatment (Fig. 3.4B) there was a significant difference when compared to the control with 3 mM METH (60.07±1.66% of control, **P<0.01; n=17). However, 24 h after METH treatment (Fig. 3.4C) a significant decrease in nitrites was observed with 1 mM or 3 mM METH (59.29±7.70% or 61.85±6.43%, **P<0.01, n=4 or n=5).

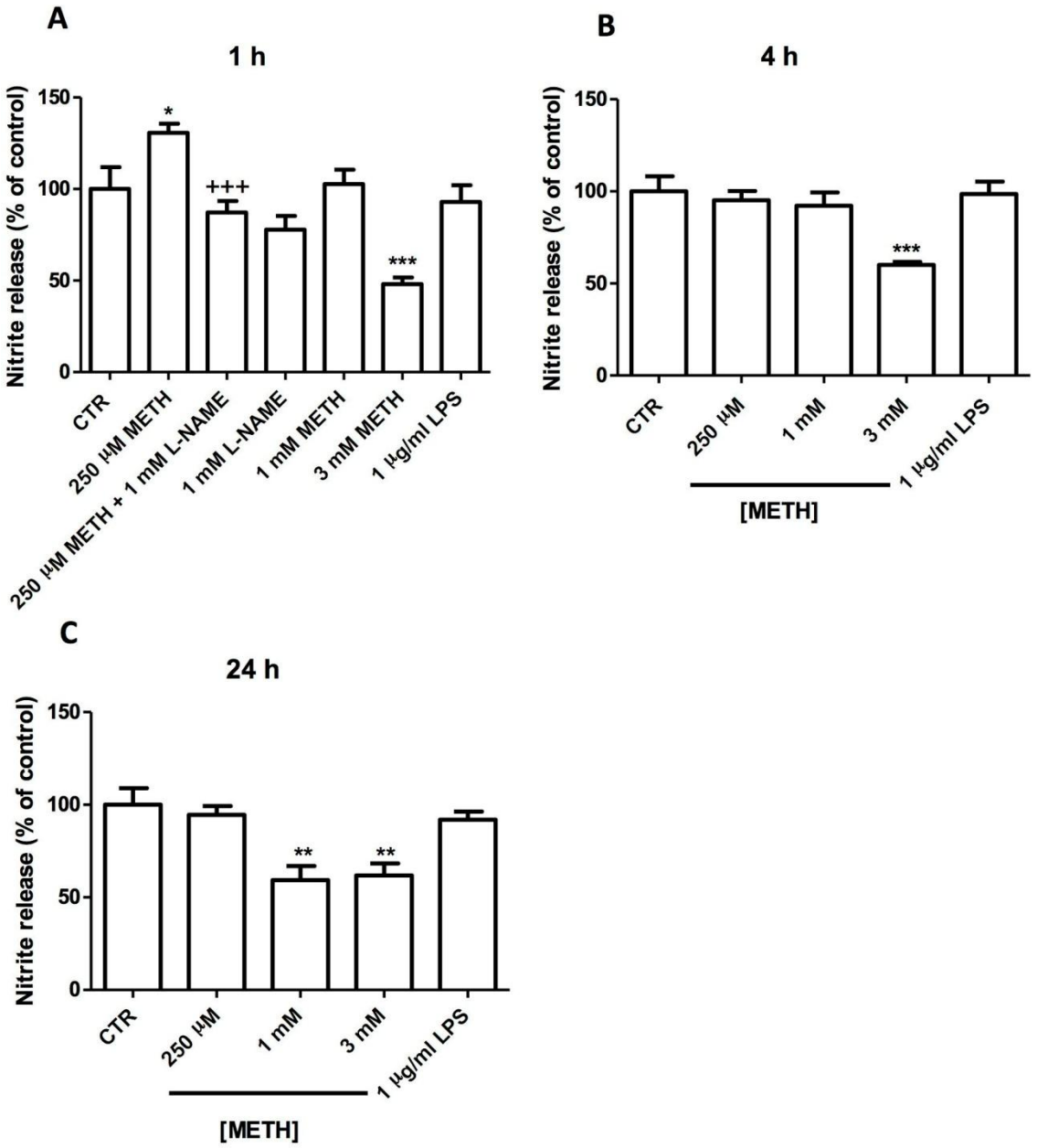

Figure 3.4 - Nitrites production by endothelial cell line bEnd.3 induced by METH at **(A)** 1 h, **(B)** 4 h and **(C)** 24 h. METH (3 mM) significantly decreased nitrites production. The results are expressed as mean percentage of control (±SEM), n=4-20. **P<0.01, ***P<0.001; significantly different from control using Dunnett´s post-test. +++P<0.001, significantly different from 1 µM METH using Bonferroni´s post-test.

3.2 Effect of METH on endothelial and microglial cell viability

We have previously in this study showed that METH leads to an increase in nitrite levels, 1 h after METH treatment, with no significant alterations at other time points.

Thus, to clarify if the increased levels of nitrites could be related with cell alterations, we further evaluated the viability of microglial cells at the three time-points previously evaluated, when exposed to 1, 10 or 100 µM METH.

Although, our study show that METH concentrations used, at the previously studied time points, are not able to induce any alteration on N9 cells viability (Fig. 3.5).

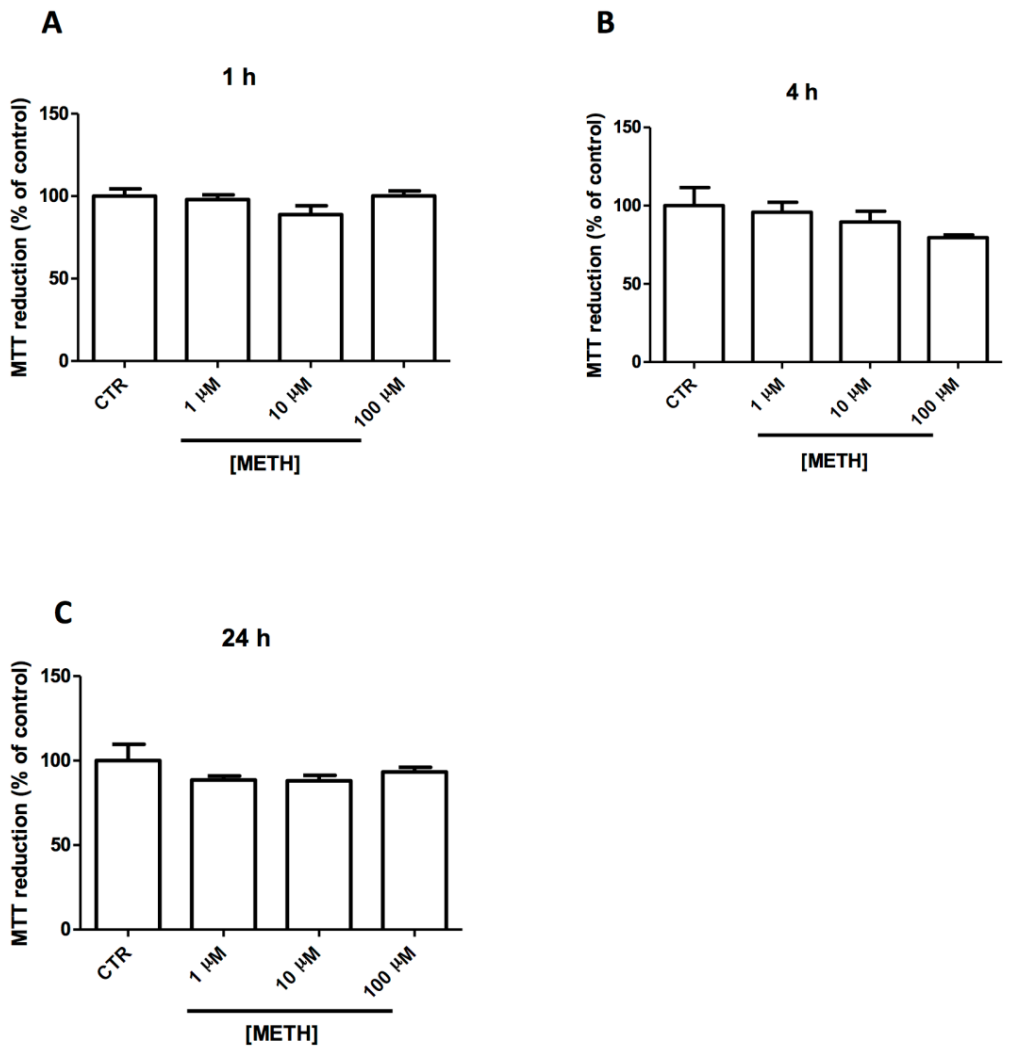

Figure 3.5 - METH exposure during **(A)** 1 h, **(B)** 4 h and **(C)** 24 h did not lead to an alteration in N9 viability. The results are expressed as mean percentage of control ± SEM; n= 3-9.

Concerning endothelial cells, it was shown that METH induces several deleterious effects at the BBB. In fact, some authors observe BBB disruption on brain regions such as cortex , hippocampus (Kiyatkin and Sharma, 2009) and caudate-putamen (Bowyer and Ali,

2006). Also, others clearly demonstrated that METH directly affects ECs (Ramirez *et al.*, 2009; Martins *et al.*, 2013). Thus, to clarify if the decreased levels of nitrites could be related with cell alterations, we further evaluated the viability of endothelial cells at the three time-points, when exposed to 1 mM METH (Fig. 3.6A) or 3 mM METH (Fig. 3.6B). Our results reveal a significant decrease in cell viability at 24 h with 1 mM METH (68.24±3.69% of control, **P<0.01, n=9) and also a significant decrease with 3 mM METH at 1, 4 and 24 h (63.85±5.99% of control, *P<0.05, n=7; 56.94±2.46% of control, **P<0.01, n=9 and 45.69±4.91% of control, ***P<0.001, n=9, respectively).

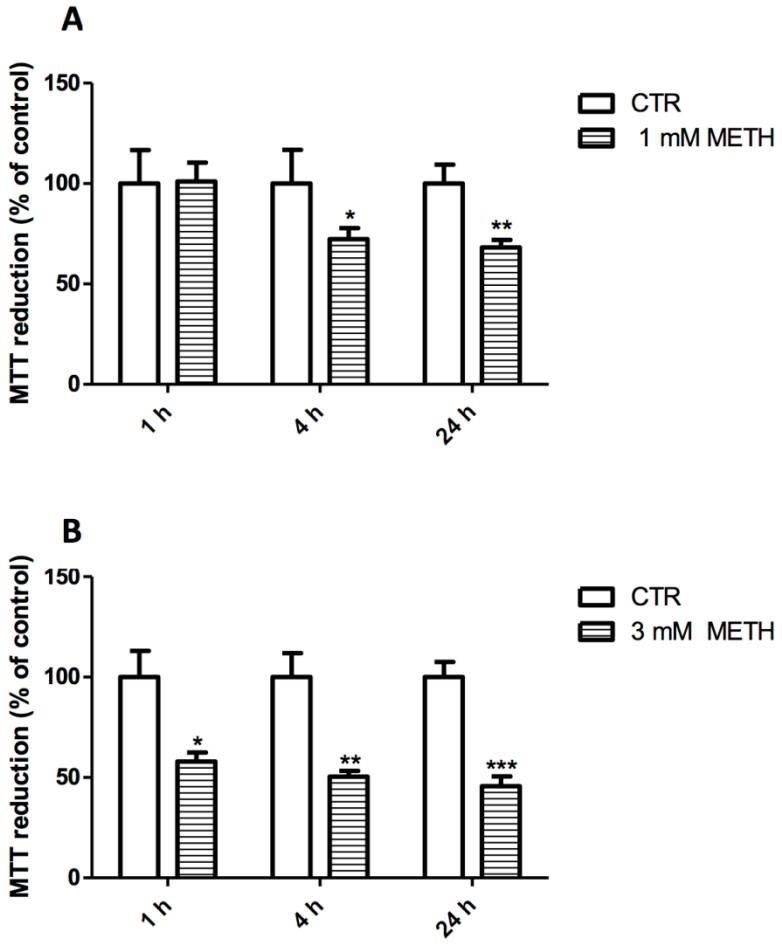

Figure 3.6 - Time-dependent effect of **(A)** 1 mM METH or **(B)** 3 mM METH on bEnd.3 cell viability. Cells were exposed to 3 or 1 mM METH for 1 h, 4 h and 24 h. The results are expressed as mean percentage of control (±SEM), n=3-9. *P<0.05;**P<0.01; ***P<0.001, significantly different from control using t-test.

3.3 METH-induced ROS production by endothelial and microglial cells

Microglial cells are the main cellular regulators of CNS homeostasis, and after an injury, microglia is rapidly activated, leading to the production of several ROS (Block *et al.*, 2007; Kraft and Harry, 2011). Since ROS are an important element in METH toxicity (Krasnova and Cadet, 2009), we further aimed to investigate if METH was able to trigger the production of ROS. For that, we used a fluorescent probe, H_2DCFDA. Different time points (1, 4 and 24 h) and different concentrations (1 µM, 10 µM and 100 µM METH) were used to cover a wide range of possible alterations.

Data obtained for 1 h and 4 h of METH exposure (Fig. 3.7A and 3.7B) show that there is no difference in ROS production induced by METH or LPS.

On the contrary, after 24 h of METH exposure (Fig. 3.7C) there was a significant increase in ROS levels with 1 µM METH (157.34±14.22% of control, n=18) or 10 µM METH (167.70±18.09; **P*<0.05; n=19) when compared to the control (control: 100.00±8.74, n=6). However, 100 µM METH and 1 µg/ml LPS did not induce a significant change in ROS production (69.39±3.36, n=19 and 88.82±8.43, n=20; respectively).

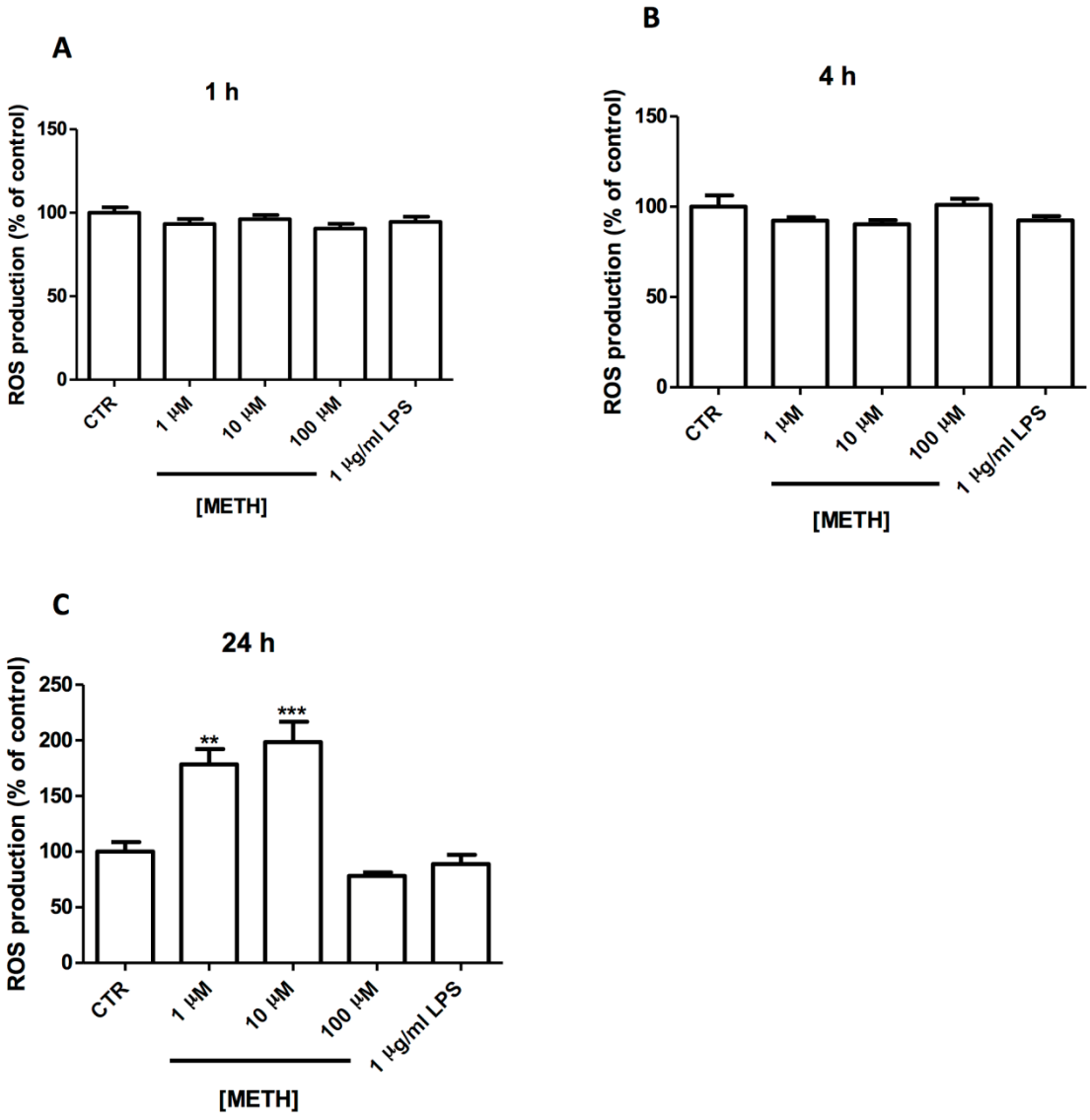

Figure 3.7 - METH effect on ROS levels in N9 cell line after **(A)** 1 h, **(B)** 4 h and **(C)** 24 h of exposure. The results are expressed as mean percentage of control ± SEM, n=4-20. *P<0.05, ***P<0.001 - Dunnet´s post-test; significantly different from the control.

It is known that METH may lead to ROS production in several brain regions, which can explain BBB disruption induced by this drug (Dietrich, 2009). Some studies have shown that METH promotes BBB disruption by induction of oxidative stress in endothelial cells (Ramirez *et al.*, 2009). Also, results from Park and colleagues (Park *et al.*, 2011) report an increase in NOX complex activity with a consequent production of ROS.

Based on these results, in the present study we also evaluated if METH could trigger ROS production by bEnd.3 cells. Once again, the fluorescent probe H_2DCFDA was used, and endothelial cells were exposed to 250 µM, 1 mM and 3 mM METH during different time points (1, 4 and 24 h). Here, we did not observed any alterations regarding ROS levels (Fig. 3.8).

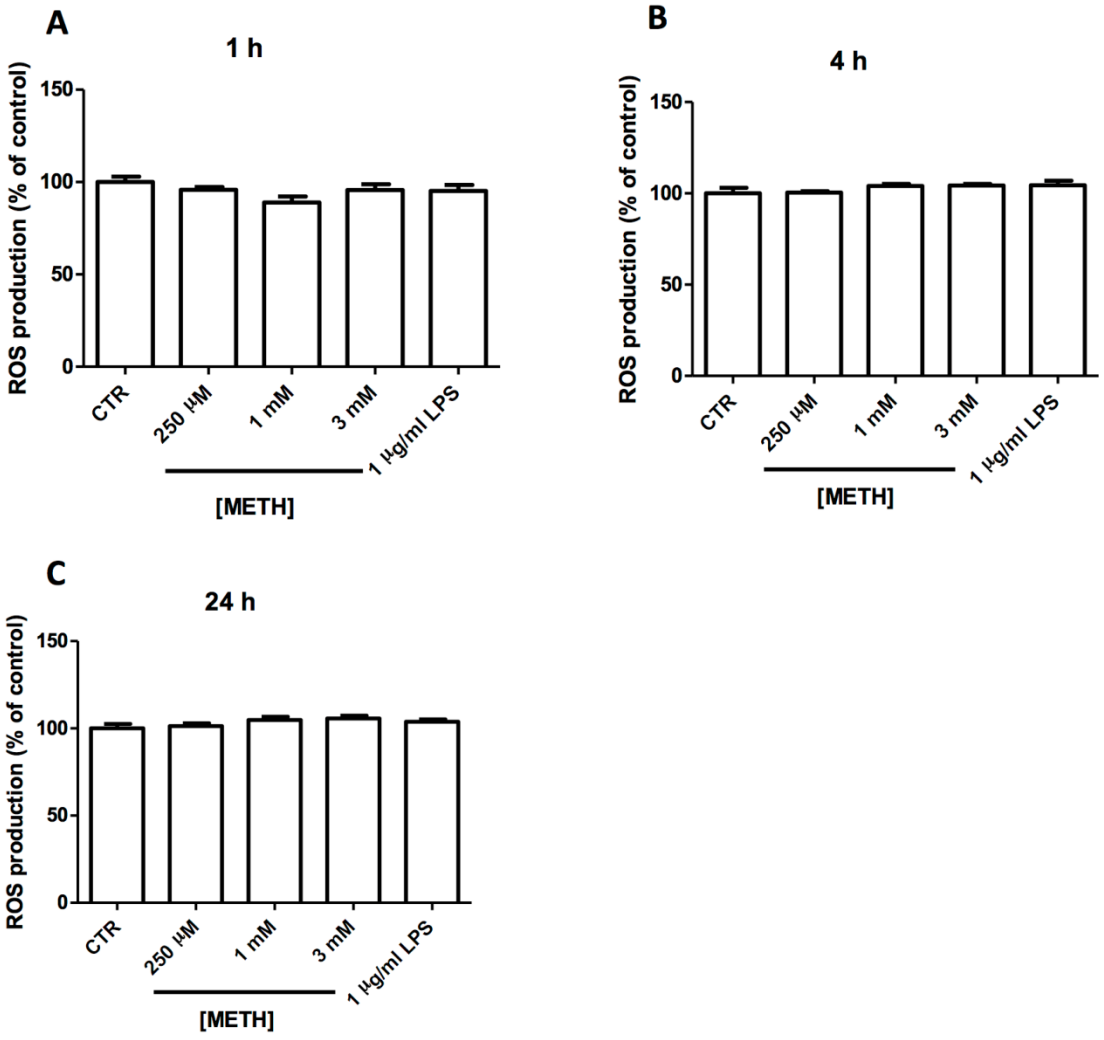

Figure 3.8 - METH effect on ROS levels in endothelial cell line bend.3 after **(A)** 1 h, **(B)** 4 h and **(C)** 24 h. The results are expressed as mean percentage of control ± SEM; n= 3-9.

Chapter 4 - Discussion

Chapter 4

Discussion

METH is a highly addictive drug of abuse and a potent central nervous system stimulant (Krasnova and Cadet, 2009). It induces damage to different cells and systems, such as dopaminergic, serotonergic and glutamatergic neurotransmission (Krasnova, 2009). Indeed, METH has several neurotoxic features that may include oxidative stress, excitotoxicity, mitochondrial dysfunction and neuroinflammation (Yamamoto and Raudensky, 2008; Krasnova and Cadet, 2009; Yamamoto *et al.*, 2010). When the homeostasis of the brain is disturbed, there is an inflammatory response involving several cells and molecules that can culminate in cell death. In fact, neuroinflammation is one of the most prominent response to CNS injury, and usually involves a complex response of all cells present in the CNS, including neurons, astrocytes and microglia. Moreover, microglial activation has already been described in the brain of METH users (Sekine *et al.*, 2008), in mouse striatum (Lavoie *et al.*, 2004) and hippocampus (Gonçalves *et al.*, 2010). These cells when activated will release a diversity of inflammatory mediators, such as chemokines, cytokines, NO and MMPs (Czeh *et al.*, 2011).

In the present study, we aimed to better clarify the inflammatory response triggered by METH in both microglial and endothelial cells. For that, we started by evaluating the release of nitrites, as an indirect measurement of nitric oxide, and LPS was used as a positive control to induce nitrite release. In fact, several studies reported that LPS induces nitrite release in microglial cells (Ferreira *et al.*, 2010; Huo *et al.*, 2011; Kacimi *et al.*, 2011; Lijia *et al.*, 2013;). Specifically, Lijia and colleagues observed a significant release of nitrite induced by 1 μg/ml LPS at different time points (1, 3, 6 and 12 h post-exposure; Lijia *et al.*, 2012). Moreover, using the same concentration of LPS, Kacimi and colleagues (2011) observed a significant increase in nitrite release 24 h after exposure. These results are in agreement with ours, since we observed an increase in nitrite levels at 1 h and 24 h post exposure. Although not statistically significant, at 4 h after LPS exposure there was a tendency to increase.

Regarding METH effects, an animal study has previously shown that METH increases nitrite levels in mice striatum at 72 h post drug administration (3x 5 mg/Kg) (Anderson and Itzhak, 2006). Here, using an *in vitro* approach, we also observed a significant increase of nitrite levels triggered by METH. In fact, we performed a time course study and concluded that METH was able to increase nitrite release by microglial cells 1 h after METH exposure. Tocharus and colleagues observed an increase in RNS but only at 6 h after METH (1.6 mM) exposure in HAPI cell line (Tocharus *et al.*, 2010). These differences can be explained by the different cells used, time of drug exposure or/and different drug concentrations. Importantly, in our study all the concentrations used did not induced cell death. However, 1.6 Mm, METH significantly decreased HAPI cells viability 24 h and 48 h post-exposure (Tocharus *et al.*, 2010). Thus, a cytotoxic response may be involved in a later NO release, whereas non-toxic concentrations induce a quick and transient response in microglial cells. Also, we only observed this effect using the lowest concentration of the drug suggesting that cell responses are somehow dependent on METH concentration. Accordingly, we have previously shown that a low concentration of METH increased endothelial cell permeability, whereas a higher concentration had no effect (Martins *et al.*, 2013). Moreover, diverse studies also demonstrated that increase in nitrite levels in microglial cells are related with increased iNOS protein levels in LPS activated cells (Kim *et al.* 2008; Lijia *et al.*, 2012). So, we can also hypothesize that METH could interfere with iNOS activity or/and levels leading to the observed increased levels of nitrites. Further studies are needed to clarify this hypothesis. Nevertheless, using a non-specific NOS inhibitor, L-NAME, it was possible to completely prevent the effect induced by METH, which further prove the involvement of NO in microglial response to METH stimuli. In fact, L-NAME has already been described to diminish nitrite release in microglial cells stimulated with LPS (Kacimi *et al.*, 2011; Lijia *et al.*, 2012), and to prevent oxidative damage to oligodendrocyte progenitor cells (OPC; Pang *et al.*, 2010).

To further evaluate the involvement of nitrergic system in microglial response mediated by METH, 3-NT levels were evaluated at the critical time point 1 h after 1 µM METH administration. NO can react with $O_2^{-\cdot}$ to produce peroxynitrite ($ONOO^-$), a highly reactive oxidant specie. Our results clearly show an increase in 3-NT staining in N9 cell line, in agreement with increased nitrite release measured with the Griess assay.

Alterations in 3-NT levels have already been reported in the mice striatum 4 h after acute METH administration (30 mg/Kg, i.p.; Wang and Angulo, 2011). Furthermore, nNOS knockout mice showed no formation of 3-NT and DA degeneration in striatum after METH administration (Imam *et al.*, 2001). Accordingly, once again we showed that L-NAME was able to inhibit 3-NT immunoreactivity induced by METH in microglial cells. Moreover, other insults besides METH have demonstrated alterations on nitrergic system of glial cells. Ryu and McLarnon showed increased hippocampal 3-NT staining in the proximity of cerebral blood vessels corresponding to microglia/macrophages and astrocytes, 7 days after $A\beta_{1-42}$ injection (Ryu and McLarnon, 2006). Also, Luth and colleagues detected nitrotyrosine in neurons, astrocytes and blood vessels in human AD patients. Interestingly, aberrant expression of nNOS in cortical pyramidal cells was highly co-localized with nitrotyrosine. Furthermore, iNOS and eNOS were highly expressed in astrocytes and co-localized with nitrotyrosine (Luth *et al.,* 2002). In the present study we did not address iNOS localization, but would be interesting to explore this issue.

After identifying a clear nitrosative stress response by microglial cells, we further aimed to identify the mechanisms involved in this effect. For that, we used a JAK/STAT pathway inhibitor (AG 490) that completely decreased nitrite release. The same was observed in BV2 cells triggered by LPS (Kacimi *et al.*, 2011). Nevertheless, besides JAK/STAT, other intracellular pathways can be involved in NO release mediated by METH, such as NF-κB and JNK that were shown to be activated by LPS in microglial cells (Kamici *et al.*, 2011). Additionally, as abovementioned, it is important to clarify that, in the present study, all METH concentrations used in microglial cells did not affect cell viability. Nevertheless, the study performed by Kacimi and colleagues suggested that NO generation was accompanied by decreased viability (Kacimi *et al*., 2011). However, investigators observed that METH diminished microglial cells viability only with concentrations similar or superior to 800 μM, in a 24 h treatment, and similar or superior to 400 μM after 48 h exposure (Tocharus *et al.*, 2010).

Besides microglia, endothelial cells have been recently shown to be highly affected by METH, and we currently know that BBB dysfunction can also be responsible for the neurotoxicity induced by METH. In fact, some studies have revealed that METH induces alterations in BBB function, which involved hyperthermia (Bowyer and Ali, 2006; Sharma

and Kiyatkin, 2009), oxidative stress (Ramirez *et al.*, 2009; Park *et al.*, 2011) and MMPs (Martins *et al.*, 2011). Additionally, NO has already been implicated in METH-induced increased BBB permeability. Therefore, as abovementioned for microglial cells, we also analyzed nitrite release by endothelial cells. The results revealed no differences when compared with the control in cells treated with LPS, at all time points analyzed. Accordingly, Kamici and collaborators (2011) treated bEnd.3 cells with 1 µg/ml LPS for 24 h and no differences were observed. However, METH (250 µM) were able to increase nitrites release but only at 1 h after drug exposure, similarly to what happened with microglia. Once again, L-NAME completely blocked this effect. Martins and colleagues (2013), using rat BMVEC, observed that METH led to barrier breakdown at 1 µM as indicated by increased EC permeability and levels of eNOS phosphorylation plateaued after 1 h. Moreover, all these effects were blocked by L-NAME reinforcing NO involvement in BBB disruption. These results, associated with the ones obtained in the present study demonstrate that NO is a key player in METH-induced toxicity.

It is well documented that METH can lead to neuronal cell death in several brain regions, such as striatum, cortex and hippocampus (Deng *et al.*, 2001, 2002), or even to microglial toxicity (Coelho-Santos *et al.*, 2011). However, the effect of METH in BBB, and more precisely on ECs, has been overlooked. Our present results show that METH has a direct time- and concentration-dependent effect on ECs viability. At a concentration of 1 mM, METH decreased cell viability only after 4 h and 24 h, without an effect at 1 h. However, 3 mM METH was able to impair endothelial cell viability just after 1 h, which was even more significant after 4 h and 24 h. This can be an explanation to the observed decrease in nitrite release, since decreased cell viability certainly affects NO release by endothelial cells. In fact, the MTT assay is used to evaluate the metabolic state of the cells, and is known that METH alters mitochondrial function. This drug is a small lipophilic molecule, and so it can easily diffuse into the mitochondria, leading to the dissipation of the electrochemical gradient established by the ETC (Davidson *et al.*, 2001), and inhibition of ATP synthesis, causing energy deficiency and subsequent mitochondrial dysfunction (Krasnova and Cadet, 2009). Another report also demonstrated that METH induced cytotoxicity in HBMVEC at a concentration of 2.5 mM, after 24 h treatment (Zhang *et al.*, 2009).

Another feature of METH-induced toxicity is the production of ROS. Thus, we further evaluate ROS production by microglial and endothelial cells in response to METH. Regarding microglial cells, our results show a significant increase in ROS production, when compared to the control, only 24 h after METH treatment. Little information is available concerning METH-induced ROS production in microglial cells. Tocharus and collaborators (2010) reported increased levels of ROS in HAPI cell line induced by METH, although they only evaluate the time point of 6 h and used a higher concentration of the drug (1.6 mM METH). Additionally, these authors used the same probe as we did (H_2DCFDA), although the concentration was 3 times higher (we used 5 µM and they used 15 µM), which could affect the sensitivity of the probe. Moreover, there is some inconsistency concerning the production of ROS induced by LPS. Huo and collaborators (2011) tested diverse time points (1, 4, 6, 12 and 24 h) and observed a significant release of ROS only at 6 h in BV2 cell line. However, in our study, no alterations were observed. These differences can be explained by the fact that different probes were used, since Huo and colleagues used the 2',7'-dichlorodihydrofluorescein diacetate (CM-H_2DCFDA)probe at 10 µM.

Finally, concerning ROS production by endothelial cells, we did not detect any changes when compared with the control. In contrast, METH (2.5 mM) was able to significantly increase ROS production in HBMVEC. Another report also demonstrated dose-dependent increase in ROS production by HBMEC exposed during 24 h to METH concentrations going from 10 to 50 µM (Ramirez *et al.*, 2009). The differences between the present work and the work of the mentioned authors may rely on the different BBB models used or also in the probes used.

Chapter 5 - Conclusions

Chapter 5

Conclusions

With the present work we concluded that METH triggers a nitrosative response on both microglial and endothelial cells, and an oxidative response on microglial cells. Moreover, the release of nitrites was prevented by the blockade of nitric oxide synthases. Importantly, these responses were induced by non-toxic concentrations of METH. Nevertheless, these effects seem to be dependent on drug concentration and time-exposure. Additionally, we also identified the involvement of JAK/STAT pathway in nitrites release. In conclusion, the present work contributes to clarify how METH affects microglial and endothelial cells.

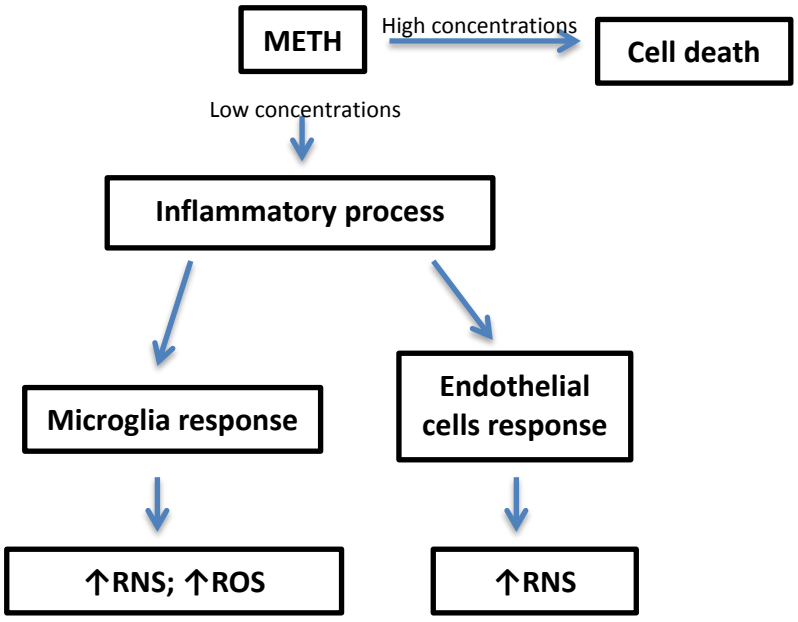

Figure 4.1 - Squematic representation of the main conclusions concerning the initial objectives.

Chapter 6 - References

Chapter 6

References

Abbott N. J., Patabendige A. A. K., Dolman D. E. M., Yusof S. R., Begley D. J. (2010) Structure and function of the blood-brain barrier. *Neurobiol Dis* **37**: 13-25.

Abbott, N., Ronnback, L. & Hansson (2006) Astrocyte-endothelial interactions at the blood-brain barrier. Nat Rev Neurosci, **7**, 41-53.

Akira, S., Takeda, K., and Kaisho,T. (2001) Toll-like receptors: critical proteins linking innate and acquired immunity. *Nat Immunol,* **2**: 675-680. Review.

Albertson T. E., Derlet, R.W. and Van Hoozen, B. E. (1999) Methamphetamine and the expanding complications of amphetamines. *West J Med*, **170**: 214-219. Review.

Alderton, W. K., Cooper, C.E. and Knowles, R.G. (2001) Nitric oxide synthases: structure, function and inhibition. *Biochem J* **357**(Pt 3): 593-615.

Ali, S. F., Newport, G. D., Holson, R. R., Slikker, W. Jr. and Bowyer, J. F. (1994) Low environmental temperatures or pharmacologic agents that produce hypothermia decrease methamphetamine neurotoxicity in mice. Brain Res., **658**: 33-38.

Anderson, K.L. and Izhak, Y. (2006) Methamphetamine-induced selective dopaminergic neurotoxicity is accompanied by an increase in striatal nitrate in the mouse. *Ann N Y Acad Sci*, **1074**: 225-233.

Anglin, M. D., Burke, C., Perrochet, B., Stamper, E. and Dawud-Noursi, S. (2000). History of the methamphetamine problem. *J Psychoactive Drugs*, **32**(2):137-41.

Babior, B.M. (199) NADPH oxidase: an update. *Blood,* **93**: 1464-1476.

Barr, A. M., Panenka, W. J., MacEwan, G. W., Thornton, A. E., Lang, D. J., Honer, W. G. and Lecomte, T. (2006) The need for speed: an update on methamphetamine addiction. *J Psychiatry Neurosci* **31**(5): 301-313. Review.

Beckman, J.S., Ye, Y.Z., Anderson, P.G., Chen, J., Accavitti, M.A., Tarpey, M.M., White, C.R. (1994) Extensive nitration of protein tyrosines in human atherosclerosis detected by immunohistochemistry. *Biol Chem Hoppe-Seyler*, **375**:81–88.

Begley, D.; Brightman, M.W. (2003) Strutural and functional aspects of the blood brain barrier. Progr Drug Res. 61:39-78.

Bento, A.R., Baptista, S., Malva, J.O., Silva, A.P. and Agasse, F. (2011). Methamphetamine exerts toxic effects on subventricular zone stem/progenitor cells and inhibits neuronal differentiation. *Rejuvenation Res*, **14**(2):205-14.

Berman, S., O'Neill, J., Fears, S., Bartzokis, G., and London, E.D. (2008). Abuse of amphetamines and structural abnormalities in the brain. *Ann N Y Acad Sci*, **1141**:195-220. Review.

Block, M.L., Zecca, L. and Hong, J.S. (2007) Microglia-mediated neurotoxicity: uncovering the molecular mechanisms. *Nat Rev Neurosci*, **8**: 57-69.

Boer, A.G., and Gaillard, P.J. (2006) Blood-brain barrier dysfunction and recovery. *J Neural Transm*, **113**: 455-462.

Bowyer, J.F. (1995) The role of hyperthermia in amphetamine´s interactions with NMDA receptors nitric oxide, and age to produce neurotoxicity. *Ann N Y Acad Sci*, **765**, 309-310.

Bowyer, J.F. and S. Ali (2006) High doses of methamphetamine that cause disruption of the blood-brain barrier in limbic regions produce extensive neuronal degeneration in mouse hippocampus, *Synapse* **60**: 521-32.

Bredt, D. S., Glatt, C.E., Hwang, P.M., Fotuhi, M., Dawson, T.M. and S. H. Snyder (1991) Nitric oxide synthase protein and mRNA are discretely localized in neuronal populations of the mammalian CNS together with NADPH diaphorase, *Neuron* **7**(4): 615-24.

Bredt, D. S., Hwang, P.M. and Snyder, S.H. (1990) Localization of nitric oxide synthase indicating a neural role for nitric oxide *Nature* **347**(6295): 768-70.

Bredt, D.S. and Snyder, S.H. (1994) Nitric oxide: a physiologic messenger molecule. *Annu Rev Biochem*, **63**: 175-95.

Brown, J.M., Quinton, M.S., Yamamoto, B.K. (2005) Methamphetamine-induced inhibition of mitochondrial complex II: roles of glutamate and peroxynitrite. *J Neurochem*, **95**: 429-436.

Burguillos, M.A., Deierborg, T., Kavanagh, E., Persson, A., Hajji, N., Garcia-Quintanilla, A., Cano, J., Brundin, P., Englund, E., Venero, JL. and Joseph, B. (2011) Caspase signalling controls microglia activation and neurotoxicity. *Nature*. **472**(7343):319-24.

Burrows, K.B., Gudelsky, G. and Yamamoto, B.K. (2000) Rapid and transient inhibition of mitochondrial function following methamphetamine or 3,4-methylenedioxymethamphetamine administration. *Eur J Pharmacol*, **398**: 11-18.

Busse, R. and Mulsch, A. (1990) Induction of nitric oxide synthase by cytokines in vascular smooth muscle cells. *FEBS Lett* **275**(1-2): 87-90.

Cadet, J.L., Ordonez, S.V. and Ordonez, J.V. (1997) Methamphetamine induces apoptosis in immortalized neural cells: protection by the proto-oncogene, bcl-2. *Synapse*, **25**(2):176-84.

Cadet, J.L. (2002) Contemporary Clinical Neuroscience: Roles of gluatamate, nitric oxide, oxidative stress and apoptosis in the neurotoxicity of methamphetamine in Herman, B.H. (Ed.), Glutamate and addition Humana Press Inc, Totowa, NJ. pp 201-210.

Cadet, J.L., Ali, S.F., Rothman, R.B. and Epstein, C.J. (1995) Neurotoxicity, drugs and abuse, and the CuZn-superoxide dismutase transgenic mice. *Mol Neurobiol*, 11(1-3): 155-163.

Cardoso, F.L., D. Brites and Brito, M.A. (2010) Looking at the blood-brain barrier: Molecular anatomy and possible investigation approaches. *Brain Res Rev*, **64**(2): 328-363.

Carson, M.; Thrash, J.; Walter, B. (2006) The cellular response in neuroinflammation: The role of leukocytes, microglia and astrocytes in neuronal death and survival. *Clin Neurosci Res,* **6**: 237–245.

Cass, W. A. and Manning, M. W. (1999) Recovery of presynaptic dopaminergic functioning in rats treated with neurotoxic doses of methamphetamine. *J Neurosci*, **19**: 7653-7766.

Cecchelli, R., Berezowski, V., Lundquist, S., Culot, M., Rentfel, M., Dehouck, M.P. and Fenart, L. (2007) Modelling of the blood-brain barrier in drug discovery and development. *Nat Rev Drug Discov* **6**(8): 650-661.

Coelho-Santos V., Gonçalves J., Fontes-Ribeiro C., Silva A.P. (2012) Prevention of methamphetamine-induced microglial cell death by TNF-α and IL-6 through activation of the JAK-STAT pathway. *J Neuroinflamm,* **9**:1-14.

Couraud, P.O. (1994) Interactions between lymphocytes, macrophages, and central nervous system cells. *J Leukoc Biol*, **3**: 407-15. Review.

Culotta E., D.E. Koshland Jr. (1992.) NO news is good news. *Science*, **258**: 1862-1865.

Cunha-Oliveira, T., Rego, A.C., Cardoso, S.M., Borges, F., Swerdlow, R. H., Macedo, T. and Oliveira, C. R. (2006). Mitochondrial dysfunction and caspase activation in rat cortical neurons treated with cocaine or amphetamine. *Brain Res*, **1089**(1): 44-54.

Czeh, M., Gressens, P. and Kaindl, A.,M. (2011) The ying and yang of microglia. *Dev Neurosci*, **33**: 199-209.

Darke, S., Kaye, S., McKetin, R. and Duflou, J. (2008) Major physical and psychological harms of methamphetamine use. *Drug Alcohol Rev.*, **27**: 253-262. Review.

Deng, X., Wang, Y., Chou, J., Cadet, J.L. (2001) Methamphetamine causes widespread apoptosis in the mouse brain: evidence from using an improved TUNEL histochemical method. *Brain Res, Mol, Brain Res*, **93**(1):64-9.

Deng X., Cai N.S., McCoy M.T., Chen W., Trush M.A., Cadet J.L., (2002) Methamphetamine induces apoptosis in an immortalized rat striatal cell line by activating the mitochondrial cell death pathway. *Neuropharmacology*, **42**:837–845.

Derlet, R.W. and Heischober, B. (1990) Methamphetamine-Stimulant of the 1990s?*West J. Med.*, **153**: 625-628. Review.

Dietrich, J.B. (2009) Alteration of brain barrier function by methamphetamine and cocaine. *Cell Tissue Res*, **336**: 385-392.

Dijkstra, G., Moshage, H., van Dullemen, H.M., de Jager-Krikken, A., Tiebosch, A.T., Kleibeuker, J.H., Jansen, P.L., van Goor, H. (1998) Expression of nitric oxide synthases and formation of nitrotyrosine and reactive oxygen species in inflammatory bowel disease. *J Pathol*, **186**:416–421.

Dikalov, S. (2011) Cross talk between mitochondria and NADPH oxidases. *Free Radic Biol Med*, **51**:1289-1301. Review.

Dilger, R.N. and Johnson, R.W. (2008) Aging, microglial cell priming, and the discordant central inflammatory response to signals from the peripheral immune system. *J Leukoc Biol*, **84**(4):932-9.

Donaldson, M. and Goodchild, J. H. (2006) Oral health of the methamphetamine abuser. *Am J Health-Syst Pharm*, **63**(21): 2078-2082.

Dziennis S., Alkayed N.J. (2008) Role of signal transducer and activator of transcription 3 in neuronal survival and regeneration. *Rev Neurosci*, **19**(4-5): 341-61. Review.

Farooqui, A.A., Horrocks, L.A. and Farroqui, T. (2007) Modulation of inflammation in brain: a matter of fat. *J Neurochem*, **101**: 577-599.

Ferreira, R., Xapelli, S., Santos, T., Silva, A.P., Cristóvão, A., Cortes, L. and Malva, J.O. (2010) Neuropeptide Y modulation of interleukin-1{beta} (IL-1{beta})-induced nitric oxide production in microglia. *J Biol Chem*, **285**(53): 41921-34.

Fleckenstein, A. E., Volz, T. J., Riddle, E. L., Gibb, J. W. and Hanson, G. R. (2007) New insights into the mechanism of action of amphetamines. *Ann Rev Pharmacol Toxicol*, **47**: 681-698. Review.

Frei, K., Lins, H., Schwerdel, C. and Fontana, A. (1994) Antigen presentation in the central nervous system. The inhibitory effect of IL-10 on MHC class II expression and production of cytokines depends on the inducing signals and the type of cell analyzed. *J Immunol*, **152**(6): 2720-2728.

Friedman, S. D., Castañeda, E. and Hodge, G.K. (1998) Long-term monoamine depletion, differential recovery, and subtle behavioral impairment following methamphetamine-induced neurotoxicity. *Pharmacol Biochem Behav*, **61**: 35-44.

Garthwaite, J., Charles, S.L. and Chess-Williams, R. (1988) Endothelium-derived relaxing factor release on activation of NMDA receptors suggests role as intercellular messenger in the brain. *Nature,* **336**(6197): 385-388.

Garthwaite, J., Garthwaite, G., Palmer, R.M. and Moncada, S. (1989) NMDA receptor activation induces nitric oxide synthesis from arginine in rat brain slices. *Eur J Pharmacol,* **172**(4-5): 413-416.

Gluck, M.R., Moy, L. Y., Jayatilleke, E., Hogan, K.A., Manzino, L. and Sonsalla, P. K. (2001) Parellelel increses in lipid and protein oxidative markers in several mouse brain regions after methamphetamine treatment. *J Neurochem*, **79**: 152-160.

Gonçalves, J., Martins, T., Ferreira, R., Milhazes, N., Borges, F., Ribeiro, C., Malva, J., Macedo, T., Silva, A. (2008) Methamphetamine-induced early increase of IL-6 and TNF-alpha mRNA expression in the mouse brain. *Ann N Y Sci* **1139**: 103-111.

Gonçalves, J.; Baptista, S.; Martins, T.; Milhazes, N.; Borges, F.; Ribeiro, C.; Malva, J.; Silva, A. (2010) Methamphetamine-induced neuroinflammation and neuronal dysfunction in the mice hippocampus: preventive effect of indomethacin. *Eur J Neurosci* **31**: 315-326.

Gordon, S. (2002) Pattern recognition receptors: doubling up for the innate response. *Cell*, **111**: 927-930.

Gorina, R., Sanfeliu, C., Galitó, A., Messeguer, À. And Planas, A.M. (2007) Exposure of glia to pro-oxidant agents revealed selective Stat1 activation by H_2O_2 and Jak2-independent antioxidant features of the Jak2 inhibitor AG490. *Glia*, **55**(13): 1313-1324.

Hanisch, U.K. Kettenmann, H. (2007) Microglia: active sensor and versatile effector cells in the normal and pathologic brain. *Nat Neurosc,* **10**: 1387-1394.

Harvey, D.C., Lacan, G., Tanious, S. P. and Melega, W. P.(2000) Recovery from methamphetamine induced long-term nigrostriatal dopaminergic deficits without substantia nigra cell loss. *Brain Res*, **871**: 259-270.

Hauwel, M., Furon, E., Canova, C., Griffiths, M., Neal, J. and Gasque, P. (2005) Innate (inherent) control of brain infection, brain inflammation and brain repair: the role of microglia, astrocytes, "protective" glial stem cells and stromal ependymal cells. *Brain Res Rev*, **48**: 220-233.

Hawkins, B.T. and Davis, T.P. (2005) The Blood-Brain Barrier/Neurovascular Unit in Health and Disease. *Pharmacol Rev,* **57**(2): 173-85.

Heim, M.H. (1999) The JAK-STAT pathway: cytokine signalling from the receptor to the nucleus. *J Signal Transduct Res*, **19**(1-4): 75-125.

Hevel, J. M., White, K.A. and Marletta, M.A. (1991) Purification of the inducible murine macrophage nitric oxide synthase. Identification as a flavoprotein. *J Biol Chem,* **266**(34):22789-91.

Hisanaga, K., Asagi, M., Itoyama, Y. and Iwasaki, Y. (2001) Increase in peripheral CD4 bright+CD8 dull+ Tcells in Parkinson disease. *Arch Neurol*, **58**: 1580-1583.

Hogan, K. A., Staal, R. G., Sonsalla, P. K.(2000) Analysis of VMAT2 binding after methamphetamine or MPTP treatment: disparity between homogenates and vesicle preparations. *J Neurochem*, **74**: 2217-2220.

Homer, B. D., Solomon, T. M., Moeller, R. W., Mascia, A., DeRaleau, L. and Halkitis, P.N. (2008). Methamphetamine abuse and impairment of social functioning: a review of the underlying neurophysiological causes and behavioral implications. *Psychol Bull*, **134**: 301–310. Review.

Huang, C., Ma, R., Sun, S., Wei, G., Fang, Y., Liu, R. and Li, G. (2008) JAK2/STAT3 signaling pathway mediates thrombin-induced proinflammatory actions of microglia *in vitro*. *Journal of Neuroimmunology* **204**: 118-125.

Huber, J. D., Egleton, R. D. and Davis,T. P. (2001) Molecular physiology and pathophysiology of tight junctions in the blood-brain barrier. *Trends Neurosci*, **24**(12): 719-725. Review.

Huo, Y., Rangarajan, P., Ling, E. and Dheen, S.T. (2011) Dexamethasone inhibits the Nox dependent ROS production via suppression of MKP-1-dependent MAPK pathways in activated microglia. *BMC Neuroscience*, **12**: 49.

Imam, S.Z., Itzhak, Y., Cadet, J.L., Islam, F., Slikker, W. Jr. and Ali, S.F. (2001). Methamphetamine-induced alteration in striatal p53 and bcl-2 expressions in mice. Brain Res *Mol Brain Res*., **91**(1-2):174-8.

Iwashita, A., Mihara, K., Yamazaki, S., Hattori, K., Matsuoka, N., Mutoh, S. (2004) A new poly(ADP-ribose) polymerase inhibitor, FR261529 [2-(4-chlorophenyl)-5-quinoxalinecarboxamide], ameliorates methamphetamine-induced dopaminergic neurotoxicity in mice. *J Pharmacol Exp Ther*, **310**(3):1114-24.

Instituto da Droga e da Toxicodependência (IDT), I.P. (2011), Relatório anual 2011. A situação do país em matéria de drogas e toxicodependências, IDT, Lisboa.

Itzhak, A., Ali, S.F. (2006) Role of nitrergic system in behavioral and neurotoxic effects of amphetamine analogs. *Pharmacol Exp Ther*, **109**, 246-262.

Ischiropoulos, H., Gow, A., Thom, S.R., Koo,y N.W., Royall, J.A., Crow, J.P (1999) Detection of reactive nitrogen species using 2,7-dichlorodihydrofluorescein and dihydrorhodamine 123. *Methods Enzymol*, **301**:367–373.

LaVoie, M.J., Card, J.P. and Hastings, T.G. (2004) Microglial activation precedes dopamine terminal pathology in methamphetamine-induced neurotoxicity, *Exp Neurol*, **187**: 47-57.

Matsuura, S., Ishida, J., Yamamoto, H., Iztak, Y. and Ali, S. K. (2006) Role of nitrergic system in behavioral and neurotoxic effects of methamphetamines analogs. *Pharmacol Ther*, *109*, 246-262.

Jayanthi, S., Deng, X., Bordelon, M., McCoy, M.T. and Cadet J.L. (2001) Methamphetamine causes differential regulation of pro-death and anti-death Bcl-2 genes in the mouse neocortex. *FASEB J*, **15**(10):1745-52.

Jayanthi, S., Deng, X., Noailles, P.A., Ladenheim, B. and Cadet, J. L. (2004) Methamphetamine induces neuronal apoptosis via cross-talks between endoplasmic reticulum and mitochondria-dependent death cascades. *FASEB J*, **18**: 238-251.

Jiménez, A., Jordà, E.G., Verdaguer, E., Pubill, D., Sureda, F.X., Canudas, A.M., Escubedo, E., Camarasa, J., Camins, A. and Pallàs, M. (2004) Neurotoxicity of amphetamine derivatives is mediated by caspase pathway activation in rat cerebellar granule cells. *Toxicol Appl Pharmacol*, **196**(2):223-34.

Kacimi, R., Giffard, R.G. and Yerani, M.A. (2011) Endotoxin-activated microglia injure brain derived endothelial cells via NF-κB, JAK/STAT and JNK stress kinase pathways. *Journal of Inflammation*, **8**:7

Kim, H.S., Cho, I.H., Kim, J.E., Shin, Y.J., Jeon, J.H., Kim, Y., Young, M.Y., Lee, K.H., Lee, J.W., Lee, W.J., Ye, S. and Chung, M. (2008) Ethyl pyruvate has an anti-inflammatory effect by inhibiting ROS-dependent STAT signaling in activated microglia. *Free Radical Biology & Medicine 45*:950-963.

Kim, S.U. and de Vellis, J. (2005) Microglia in health and disease. *J Neurosci Res*, **81**: 302-313.

Kim, O.S. Park, E.J.,Joe, E.H. and Jou, I. (2002) JAK-STAT signaling mediates gangliosides-induced inflammatory responses in brain microglial cells. *J Biol Chem*, **277**(43): 40594-601.

Kish, S.J. (2008) Pharmacological mechanism of crystal meth. *CMAJ*, **178**:1679-1682.

Kishimoto, T., Taga, T., Akira, S., (1994) Cytokine signal transduction. *Cell* **76**: 253–262.

Kiyatkin, E.A. and Sharma, H.S. (2009) Acute methamphetamine intoxication: brain hyperthermia, blood-brain barrier, brain edema and morphological cell abnormalities. *Int Rev Neurobil*, **88**: 65-100.

Klongpanichapak, S., Govitrapong, P., Sharma, S.K. and Ebadi, M. (2006) Attenuation of cocaine and methamphetamine neurotoxicity by coenzyme Q10. *Neurochem Res*, **31**: 303-311.

Kocherginsky, N. (2000) Acidic lipids, Hþ-ATPases, and mechanism of oxidative phosphorylation. Physico-chemical ideas 30 years after P. Mitchell's Nobel Prize award. *Prog Biophys Mole Bioly*, **99**:20-41. Review.

Kraft, A.D., Harry, G.J. (2011) Features of microglia and neuroinflammation relevant to environmental exposure and neurotoxicity. *Int J Environ Res Public Health,* 8(7): 2980-3018.

Krasnova, I., Cadet, J. (2009) Methamphetamine toxicity and messengers of death. *Brain Res Rev* **60**(2): 379-407.

Lijia, Z., Siqi, Z., Xiaoxiao, W., Chunfu, W. and Jingyu, Y. (2012) A self-proliferating cycle mediated by reactive oxide species and nitric oxide exists in PLS-activated microglia. *Neurochem int*, **61**: 1220-1230.

Lucas, S.M., Rothwell, N.J. and Gibson, R.M. (2006) The role of inflammation in CNS injury and disease. Br J Pharmacol, **147 Suppl 1**: S232-240.

Lull, M.E., Block, M.L. (2010) Microglial activation and chronic degeneration. *Neurotherapeutics* **7**(4): 354-65.

Luth, H., Munch, G. and Arendt, T. (2002) Aberrant expression of NOS isoforms in Alzheimer's disease isstructurally related to nitrotyrosine formation. *Brain* Res, **953**: 135-143.

MacMicking, J., Xie, Q.W. and Nathan, C. (1997) Nitric oxide and macrophage function. *Annu Rev Immunol*, **15**: 323-350.

Mahajan, S.D., Aalinkeel, R., Sykes,D.E., Reynolds, J.L, Bindukumar, B., Adal, A., Qi, M., Toh, Xu, J.G., Prasad, P.N. and S.A. Schwartz, S.A. (2008) Methamphetamine alters blood brain barrier permeability via the modulation of tight junction expression: Implication for HIV-1 neuropathogenesis in the context of drug abuse. *Brain Res* **1203**: 133-48.

Marshall J. F. and O'Dell S. J., (2012) Methamphetamine influences on brain and behavior: unsafe at any speed? *Trends Neurosci*. **35**:536-45.

Martins, T., Baptista, S., Gonçalves, J., Leal, E., Milhazes, N., Borges, F., Ribeiro, C.F., Quintela, O., Lendoiro, E., López-Rivadulla, M., Ambrósio, A.F. and Silva, A.P. (2011) Methamphetamine transiently increases the blood-brain barrier permeability in the hippocampus: role of tight junction proteins and matrix metalloproteinase-9. *Brain Res*, **1411**: 28-40.

Martins T., Burgoyne T., Kenny B., Hudson N., Futter C. E., Ambrósio A. F., Silva A. P., Greenwood J., Turowski P. (2013) Methamphetamine-induced nitric oxide promotes vesicular transport in blood-brain barrier endothelial cells. *Neuropharmacology* **65**: 74-82.

Meredith, C. W., Jaffe, C., Ang-Lee, K., and Saxon, A. J. (2005) Implications of Chronic Methamphetamine Use: A Literature Review. Harv Rev *Psychiatry*, **13**(3): 141-154.

Montesano, R., M. Pepper, U. Mohle-Steinlein, W. Risau, E. Wagner and L. Orci (1990) Increased proteolytic activity is responsible for the aberrant morphogenetic behavior of endothelial cells expressing the middle T oncogene. *Cell*, **62**: 435-45.

Mosmann, T. (1983) Rapid colorimetric assay for cellular growth and survival: application to proliferation and cyto-toxicity assays. *J Immunol Methds,* **65**: 55-63.

Muller, F. (2000) The nature and mechanism of superoxide production by the electron transport chain: Its relevance to aging. ***J Am Aging Assoc*** , 23(4)**: 227–253.**

Munneer, A., Alikunju, S., Szlachetka, A.M., Murrin, L.C. and Haorah, J. (2011) Impairment of brain endothelial glucose transporter by methamphetamine causes blood-brain barrier dysfunction. Mol Neurodegener, **6**: 23.

Nakamura, Y. (2002) Regulating Factors for Microglial Activation, Biol. *Pharm Bull*, **25**:945-953.

Nash, J. F. and Yamamoto, B. K. (1992) Methamphetamine neurotoxicity and striatal glutamate release: comparison to 3, 4-methylenedioxymethamphetamine. *Brain Res*, **581**: 237-243.

Nguyen, M.D., Julien, J.P. and Rivest, S. (2002) Innate immunity: the missing link in neuroprotection and neurodegeneration? *Nat Rev Neurosci*, **3**: 216-227.

Palmer, R.M., D.S. Ashton and S. Moncada (1988) Vascular endothelial cells synthesize nitric oxide from L-arginine, Nature **333**(6174): 664-6.

Pang, Y., Campbell, B., L., Fan, L., Cai, Z. and Rhodes, P. (2010) Lipopolysaccharide-activated microglia induce death of oligodendrocyte progenitor cells and impede their development. *Neuroscience,* **166**(2): 464-475.

Park, J.I., Strock, C.J., Ball, D.W. and Nelkin, B.D. (2003)The Ras/Raf/MEK/extracellular signal-regulated kinase pathway induces autocrine-paracrine growth inhibition via the leukemia inhibitory factor/JAK/STAT pathway. *Mol Cell Biol*, **23**(2):543-54.

Park, K.M. and Bowers, W.J. (2010) Tumor necrosis factor-alpha mediated signaling in neuronal homeostasis and dysfunction. *Cell Signal*, **22**: 977-983.

Perez, J. A. Jr., Arsura, E. L. and Strategos, S. (1999). Methamphetamine-related stroke: four cases. *J Emerg Med*,. **17**(3):469-71.

Persidsky, Y., S.H. Ramirez, J. Haorah and G.D. Kanmogne (2006) Blood-brain barrier: Structural components and function under physiologic and pathologic conditions. *J Neuroimmune Pharmacol* **1**: 223-36.

Prast, H. and Philippu, A. (2001) Nitric oxide as modulator of neuronal function *Prog Neurobiol* **64**(1): 51-68.

Quinton, M.S. and Yamamoto, B.K. (2006) Causes and consequences of methamphetamine and MDMA toxicity (2006). *AAPS J*, **8**, E337-347.

Ramirez, S. H., Potula, R., Fan, S., Eidem, T., Papugani, A., Reichenbach, N., Dykstra, H., Weksler, B.B., Romero, I.A., Couraud, P.O. and Perdidsky, Y. (2009) Methamphetamine disrupts blood-brain barrier function by induction of oxidative stress in brain endothelial cells . *J Cereb Blood Flo Metab* **29**: 1933-45.

Rawlings, J.S., Rosler, K.M., and Harrison, D.A. (2004) The JAK/STAT signalling pathway. *J cell Sci,* 117: 1281-1283.

Ribic, A., Zhang, M., Schlumbohm, C., Matz-Rensing, K., Uchaska-Ziegler, B., Flugge, G., Zhang, W., Walter, L. and Fuchs, E. (2010) Neuronal MHC class I molecules are involved in excitatory synaptic transmission at the hippocampal mossy fiber synapses of marmoset monkeys. *Cell Mol Neurobiol*, **30**: 827-839.

Ricaurte, G. A., Guillery, R. W., Seiden, L.S., Schuster, C.R. and Moore, R.Y. (1982) Dopamine nerve terminal degeneration produced by high doses of methylamphetamine in the rat brain. *Brain Res*, **235**(2): 93–103.

Ricaurte, G., A. and McCann, U. D. (1992) Neurotoxic amphetamine analogues: effects in monkeys and implications for humans. *Ann NY Acad Sci*, **648**: 371-338. Review.

Righi, M., Mori, L., De Libero, G., Sironi, M., Biondi, A., Mantovani, A., Donini, SD. and Ricciardi-Castagnoli, P. (1989) Monokine production by microglial cell clones. *Eur J Immunol* **8**:1443-1448.

Rose, M., and Grant, J. (2008). Pharmacotherapy for methamphetamine dependence: A review of the pathophysiology of methamphetamine addiction and the theoretical basis and efficacy of pharmacotherapeutic interventions. *Ann Clin Psychiatry*, **20**(3): 145-155.

Ryu, J.K., and McLarnon, J.G. (2006) Minocycline or iNOS inhibition block 3-nitrotyrosine increases and blood –brain barrier leakin ess in amyloid beta-peptide-injected rat hippocampus. *Exp Neurol,* 198: 552-557.

Sandoval, K. and Witt, K. (2008) Blood-brain barrier tight junction permeability and ischemic stroke. *Neurobiol Dis* **32**: 200-219.

Schmidt,H., Pollock,H.J.S., Nakane, M., Gorsky, L.D., Forstermann U. and Murad, F. (1991). Purification of a soluble isoform of guanylyl cyclase-activating-factor synthase. *Proc Natl Acad Sci USA*, **88**(2): 365-9.

Seiden, L.S., Commins, D.L., Vosmer, G., Axt, K. and Marek, G. (1988). Neurotoxicity in dopamine and 5-hydroxytryptamine terminal fields: a regional analysis in nigrostriatal andmesolimbic projections. *Ann N Y Acad Sci*, **537**: 161–172. Review.

Sekine, Y., Ouchi, Y., Takei, N., Yoshikawa, E., Nakamura, K., Futatsubashi, M., Okada, H., Minabe, Y., Suzuki, K., Iwata, Y., Tsuchiya, K. J., Tsukada, H., Iyo, M. and Mori, N. (2006) Brain serotonin transporter density and aggression in abstinent methamphetamine abusers. *Arch Gen Psychiatry***, 63**: 90-100.

Gold, M. S. and Cadet, J.L. (2008) Methamphetamine causes microglial activation in the brains of human abusers. *J Neurosci*, **28**: 5756-5761.

Sharma, H., Kiyatkin, E. (2009). Rapidmorphological brain abnormalities during acute methamphetamine intoxication in the rat: an experimental study using light and electron microscopy. *J Chem Neuroanat* **37**: 18-32.

Shuai, K., Liu, B. (2003) Regulation of JAK/STAT signaling in the immune system. *NAT REV IMMUNOL* **3**: 900-911. Review.

Simões, P.F., Silva, A.P., Pereira, F.C., Marques, E., Milhazes, N., Borges, F., Ribeiro, C.F. and Macedo, T.R. (2007). Methamphetamine induces alterations on hippocampal NMDA and AMPA receptor subunit levels and impairs spatial working memory. *Neuroscience*, **150**(2):433-41.

Smith, K.J., Butler, T.R. and Prendergast, M.A. (2010) Inhibition of sigm-1 receptor reduces N-methyl-D-aspartate induced neuronal injury in methamphetamine-exposed and –naive hippocampi. *Neurosci Lett*, **481**: 144-148.

Sonsalla, P.K., Riordan, D.E. and Heikkila, R.E. (1991) Competitive and noncompetitive antagonists at N-methyl-D-aspartate receptors protect against methamphetamine-induced dopaminergic damage in mice. *J Pharmacol Exp Ther*, **256**: 506–512.

Stone, D.K., Reynolds, A.D., Mosley, R.L. and Gendelman, H.E. (2009) Innate and adaptive immunity for the pathology of Parkinson´s disease. *Antioxid Redox Signal*, **11**: 2151-2166.

Stuehr, D.J., Cho, H.J., Kwon, N.S., Weise, M.F. and Nathan, C.F. (1991) Purification and characterization of the cytokine-induced macrophage nitric oxide synthase: an FAD- and FMN-containing flavoprotein. *Proc Natl Acad Sci USA* **88**(17): 7773-7777.

Sulzer, D. and Rayport, S. (1990) Amphetamine and other psychostimulants reduce pH gradients in midbrain dopaminergic neurons and chromaffin granules: a mechanism of action. *Neuron*, **5**(6): 797-808.

Sulzer, D., Sonders, M.S., Poulsen, N.W. and Galli, A. (2005) Mechanisms of neurotransmitter release by amphetamines: A review. *Prog Neurobiol*, **75**: 406–433.

Thomas, D.; Dowgiert, J.; Geddes, T.; Fracescutti-Verbeem, D.; Liu, X.; Kuhn, D.; (2004). Microglial activation is a pharmacologically specific marker for the neurotoxic amphetamines. *Neurosci Lett* **367**: 349-354.

Thomas, D.; Francescutti-Verbeem, D. and Kuhn, D. (2008) The newly synthesized pool of dopamine determines the severity of methamphetamine-induced neurotoxicity. *J. Neurochem,.* **105**:605-616.

Thomas, D.; Kuhn, D. (2005). Cyclooxygenase-2 is an obligatory factor in methamphetamine-induced neurotoxicity*. J Pharmacol Exp Ther,* **313**: 870-876.

Thompson, P. M., Hayashi, K. M., Simon, S. L., Geaga, J. A., Hong, M. S., Sui, Y., Lee, J. Y., Toga, A.W., Ling, W. and London, E. D. (2004) Structural abnormalities in the brains of human subjects who use methamphetamine. *Neurosci*, **24** (26): 6028-6036.

Tian, C., Murrin, L.C. and Zheng, J.C. (2009) Mitochondrial fragmentation is involved in methamphetamine-induced cell death in rat hippocampal neural progenitor cells. *PLoS One*, **4**(5): e5546.

Tiskas, D. (2007) Analysis of nitrite and nitrate in biological fluids by assays based on the Griess reaction: appraisal of the Griess reaction in the L-arginine/nitric oxide area of research. *J Chromatogr B Analyt Technol Biomed Life Sci*, 851: (1-2): 51-70.

Tocharus, J., Khonthun, C., Chongthammakun, S., Govitrapong, P. (2010) Melatonin attenuates methamphetamine-induced overexpression of pro-inflammatory cytokines in microglial cell lines*. J Pineal Res*, **48**(4):347-52.

United Nations Office on Drugs and Crime (UNODC) (2012) World Drug Report. UNODC, Vienna.

Urrutia A., Rubio-Araiz A., Gutierrez-Lopez M. D., ElAli A., Hermann D.M., O'Shea E., Colado M. I., 2013. A study on the effect of JNK inhibitor, SP600125, on the disruption of blood–brain barrier induced by methamphetamine. *Neurobiol Di,s* **50**:49-58.

Volkow, N. D., Chang, L., Wang, G. J., Fowler, J. S., Franceschi, D., Sedler, M., Gatley, S. J., Miller, E., Hitzemann, R., Ding, Y. S. and Logan, L. (2001) Loss of dopamine transporters in methamphetamine abusers recovers with protracted abstinence. *J Neurosci*, **21**(23): 9414-9418.

Wagner, G.C., Ricaurte, G.A., Seiden, L.S., Schuster, C.R., Miller, R.J. and Westley J. (1980) Long-lasting depletions of striatal dopamine and loss of dopamine uptake sites following repeated administration of methamphetamine. *Brain Res*, **181**(1):151-60.

Walter, L. and Neuman, H. (2009) Role of microglia in neuronal degeneration and regeneration. *Semin Immunopathol*, **31**: 513-525.

Wang, C., Shuaib, A. (2007) Critical role of microvasculature basal lamina in ischemic brain injur. *Prog. Neurobiol.* **83**: 140-148.

Wang, J. and Angulo, J.A. (2011) Synergism between methamphetamine and the neuroptide substance P on the production of nitric oxide in the striatum of mice. *Brain Res*, **1369**: 131-139.

Wilson, J.M., Kalasinsky, K.S., Levey, A.I., Bergeron, C., Reiber, G.,Anthony, R.M., Schmunk, G.A., Shannak, K., Haycock J.W., Kish , S.J. (1996) Striatal dopamine nerve terminal markers in human, chronic methamphetamine users. *Nature Med* **2**:699–703

Warren, M.W., Larner, S.F., Kobeis sy, F.H., Brezing, C.A., Jeung, J.A.,Hayes, R.L., Gold, M.S., Wang, K.K. (2007) Calpai n and caspaseproteolytic markers co-localize w ith rat cortical neuro ns afterexposure to methamp hetamine and MDMA. *Acta Neuropathol* **114**:277-286.

Wong, D., Prameya, R. and Dorovini-Zis, K. (1999) In vitro adhesion and migration of T lymphocytes across monolayers of human brain microvessel endothelial cells: regulation by ICAM-1, VCAM-1, E-selectin and PECAM-1**.** *J Neuropathol Exp Neurol*, **58**(2): 138-52.

Wu, C. W., Ping, Y. H., Yen, J. C., Chang, C.Y., Wang, S.F., Yeh, C.L., Chi, C.W. and Lee, H. C. (2007) Enhanced oxidative stress and aberrant mitochondrial biogenesis in human neuroblastoma SH-SY5Y cells during methamphetamine induced apoptosis. *Toxicol Appl Pharmacol*, **220**: 243-251.

Yamagata, K., Tagami, M., Takenaga, F., Yamori, Y. and Itoh, S. (2004) Hypoxia-induced changes in tight junction permeability of brain capillary endothelial cells are associated with IL-1beta and nitric oxide. *Neurobiol Dis,* **17**:491-499.

Yamamoto, B. K., Moszczynska, A. and Gudelsky, G. A. (2010) Amphetamine toxicities: classical and emerging mechanisms. *Ann N Y Acad Sci*, **1187**: 101-121. Review.

Yamamoto, B.K. and Raudensky, J. (2008). The role of oxidative stress, metabolic compromise, and inflammation in neuronal injury produced by amphetaminerelated drugs of abuse. *J Neuroimmune Pharmacol*, **3**: 203-217. Review.

Zhu, P., Hata, R., Cao, F., Gu, F., Hanakawa, Y., Hashimoto, K. and Sakanaka, M. (2008)Ramified microglial cells promote astrogliogenesis and maintenance of neural stem cells through activation of Stat3 function. *FASEB J*, **22**(11):3866-77.